This is to certify that the

dissertation entitled

One-Dimensional Acoustic Response with Mixed Boundary Condition: Separating Total Response Into Propagating and Standing Wave Components

presented by

Charles E. Spiekermann

has been accepted towards fulfillment of the requirements for

DOCTOR OF PHILOSOPHY degree in MECHANICAL ENGINEERING

Clark Radcliffe
Major professor
Clark J. Radcliffe
Associate Professor

Date May 13, 1986

PLACE IN RETURN BOX to remove this checkout from your record.
TO AVOID FINES return on or before date due.

DATE DUE	DATE DUE	DATE DUE
~~FEB 2 1998~~ JUN 10 1999 442		

MSU Is An Affirmative Action/Equal Opportunity Institution
c:\circ\datedue.pm3-p.1

One-Dimensional Acoustic Response with Mixed Boundary Condition: Separating Total Response Into Propagating and Standing Wave Components

By

Charles E. Spiekermann

A DISSERTATION

Submitted to
Michigan State University
in partial fulfillment of the requirements
for the degree of

DOCTOR OF PHILOSOPHY

Department of Mechanical Engineering

1986

This is to certify that the
dissertation entitled

One-Dimensional Acoustic Response with Mixed
Boundary Condition: Separating Total Response
Into Propagating and Standing Wave Components

presented by

Charles E. Spiekermann

Charles E. Spiekermann

5-9-86

Charles E. Spiekermann
DOCTOR OF PHILOSOPHY Candidate

Date

has been accepted towards fulfillment
of the requirements for
a
DOCTOR OF PHILOSOPHY DEGREE in Mechanical Engineering
at
Michigan State University

by

Clark Radcliffe

Clark J. Radcliffe
Associate Professor
Dissertation Advisor

May 9, 1986

Date

John R. Lloyd

John R. Lloyd
Chairman
Department of Mechanical Engineering

5-9-86

Date

ABSTRACT

One-Dimensional Acoustic Response with Mixed Boundary Condition: Separating Total Response Into Propagating and Standing Wave Components

by

Charles E. Spiekermann

Optimal design of acoustic sources and the enclosed volumes they excite require an accurate prediction of the acoustic pressure response in the enclosed volume. At one extreme, a boundary condition may be completely absorptive, resulting in a propagating wave response. An anechoic room is such an example. The other extreme is a completely reflective boundary condition, as in a reverberant room. This results in a standing wave response.

For most real systems, these two ideal boundary conditions are found in some combination. This is a mixed boundary condition. The resultant acoustic pressure response associated with a mixed boundary condition should also be a combination of the two ideal extreme responses, the propagating and standing wave responses.

Modelling the boundary condition inaccurately can lead to significant errors in the predicted total response compared to that measured in the real system. This dissertation develops a model which

includes real measurements to predict the acoustic response without requiring knowledge of the boundary condition.

A two-microphone spectral analysis technique which separates the total acoustic response into propagating and standing (STRIPS) wave components will be developed. These analytically ideal propagating and standing wave response components are extracted, or "stripped", from the measured total mixed response. Analyzing the components separately is advantageous because each is associated with an ideal boundary condition. Each is easily modelled and can be summed to obtain the total mixed response. Knowledge of the actual boundary condition is not needed.

The STRIPS method is developed for a one-dimensional system with an excitation at one end and a mixed boundary condition at the other. These components compare very well to those obtained when an analytical mixed response associated with a specified mixed boundary condition is decomposed into propagating and standing wave components. Experimental results are also compared. The experimental mixed boundary condition is obtained by matching the STRIPS method components to those obtained from the Analytical method. The derived analytical model can be used to more accurately predict the acoustic response at other locations due to an arbitrary excitation.

to Linda, with love always.

ACKNOWLEDGEMENTS

Thank you to Dr. Clark J. Radcliffe, my major advisor throughout my graduate program. His continuing friendship and encouragement led me into the doctoral program. It is an opportunity which will change the rest of my life. Our shared interests and open discussions in the past form the basis for a lasting friendship in the future.

The efforts of the other members of my Doctoral Guidance Committee, Drs. Ronald C. Rosenberg, Erik D. Goodman, and Michael Chial are greatly appreciated. Their comments concerning this dissertation were very valuable. They provided guidance and are examples for me to follow.

The A.H. Case Center for Computer-Aided Design provided laboratory space, spectral analyzers, graphics hardware, and computing time which played an integral part in the completion of this research.

To my wife, Linda. Her encouragement, strength, and support brings out the best in me. Life is more enjoyable because we are together.

My parents, Frank and Marie Spiekermann, have shown a continuing interest in my success. They have provided much moral support and are always with me in my thoughts.

The other members of my family, my brother - Richard and Carol Spiekermann and my sister - Linda and Corwin Jones, have been motivating forces in my life.

Thanks to my friends in the East Lansing area for their friendship, good times, and kind acts during the years that I have lived here.

TABLE OF CONTENTS

LIST OF FIGURES

NOMENCLATURE

A	propagating wave response amplitude
B	standing wave response scale factor
c	wave speed, m/sec
E	expected value
E_i	STRIPS residual error
G_{11}	auto-spectrum of response at $x = x_1$, N^2/m^4
G_{22}	auto-spectrum of response at $x = x_2$, N^2/m^4
G_{12}	cross-spectrum of responses at $x = x_1, x_2$, N^2/m^4
i	$\sqrt{-1}$
Im()	imaginary part
K	boundary absorptivity
L	total length, m
$P()$	acoustic pressure function, N/m^2
P_0	magnitude of pressure excitation, N/m^2
P_t	total acoustic pressure response, N/m^2
P_{1t}	total acoustic pressure response at $x = x_1$, N/m^2
P_{2t}	total acoustic pressure response at $x = x_2$, N/m^2
P_p	propagating pressure wave response component, N/m^2
P_s	standing pressure wave response component, N/m^2
Re()	real part
R_1	standing wave response amplitude at $x = x_1$, N/m^2
R_2	standing wave response amplitude at $x = x_2$, N/m^2
$R(x)$	standing wave amplitude distribution, N/m^2
S	cross-sectional area, m^2
t	time, sec
T	temperature, °C
u	acoustic particle displacement, m
x	spatial location, m
ϕ	time phase change, rad
ψ	spatial phase change, rad
ρ	density, Kg/m^3
ω	frequency, rad/sec
ω_n	natural frequency, rad/sec

A Finnish proverb goes, strong **sisu** (guts) will help get a person even through a gray rock. Now I chant "Sis-u, sis-u." inside my head as I lug myself up those weary hills toward the end of a long run.

Richard Rogin, in The Runner Magazine
and exemplified in
How to Complete and Survive a Doctoral Dissertation, David Sternberg

CHAPTER 1

INTRODUCTION

1.1 Acoustic Pressure Response

An accurate characterization of an enclosed volume's steady state acoustic pressure response is important [1] for the optimal design of both the sound excitation and the enclosed volume. This is demonstrated in audio systems, duct acoustics, and room acoustics. Sound sources, such as acoustic alarms and audio entertainment systems in automobiles, are best designed with knowledge of the acoustic pressure response of the automobile interior. Enclosed volumes may be designed to create a specific response, as in a concert hall, or to suppress acoustic response, as in a noisy factory.

An iterative prototype design process using "cut and try" methods is expensive and slow. Accurate predictions of acoustic response are needed by manufacturers to accelerate product development and to reduce design costs. Predictions of response also can be used to determine acoustic intensity and to further understanding of human perception of sound.

Many advances have been made through increased use of computer-aided design techniques that increase design productivity. Improvements in digital signal processing play a large role in this. The public interest in improved sound quality and in limiting excessive noise levels is evident, if not legislated.[2]

1.2 A New Prediction Technique

This dissertation presents a experimental-based two-microphone spectral analysis technique which separates the total acoustic response into propagating and standing (STRIPS) wave components. These analytically ideal propagating and standing wave response components are extracted, or "stripped", from the measured total mixed response. The propagating pressure component wave is absorbed at the boundary. The standing pressure wave component, due to a reflective boundary condition, contains information about the natural frequencies and mode shapes.

Analyzing the components separately is advantageous because each is associated with an ideal boundary condition. Each is easily modelled and can be summed to obtain the total mixed response. Knowledge of the actual boundary condition is not needed. It is a combination of absorptive and reflective conditions and is difficult to determine.

The STRIPS method is developed for a one-dimensional system with an excitation at one end and a mixed boundary condition at the other. The required inputs are the measured auto-spectra and cross-spectrum of the total pressure response at two locations. Results are the propagating and standing pressure wave response components, which are normalized to the excitation for convenience.

The mixed boundary condition indicates how much acoustic pressure is absorbed at the boundary, with the remainder being reflected. It is obtained by matching the STRIPS method components to those obtained from an Analytical method acoustic response model in which the mixed boundary condition is specified. The derived analytical model can be used to predict the acoustic response at other locations due to an arbitrary excitation.

1.3 Chapter Summary

Chapter 2 develops the motivation for this dissertation. Modelling acoustic pressure response accurately is discussed. The lack of accuracy in the boundary condition specification is emphasized. This may result in a large error in the predicted acoustic pressure response. Obtaining the response without requiring knowledge of the boundary condition is advantageous.

Chapter 3 develops an Analytical method for decomposing a total mixed response into propagating and standing wave components, given knowledge of the boundary condition. This is done by equating the mixed response from a one-dimensional wave equation model to scaled and phased shifted propagating and standing wave responses. This analytical approach demonstrates that the decomposition is possible. The propagating and standing wave components obtained are compared later with the STRIPS method components.

Chapter 4 develops the STRIPS method of measuring the propagating and standing wave response components, without requiring knowledge of boundary condition. A spectral analysis model is used which includes acoustic pressure measurements at two points in a one-dimensional system. This results in the propagating pressure wave component and the standing pressure wave components at the two measurement points.

Chapter 5 presents experimental results input to the STRIPS method of measuring propagating and standing wave components in a tube. Most of the pressure wave is reflected at the open tube end. This portion creates a standing wave in the tube. However, some of the sound pressure escapes out the tube end, i.e., is absorbed at the boundary. These results are compared to the Analytical method results. Common standing wave tube phenomena is evident by comparisons to analytical results. Future enhancements are noted.

Chapter 6 concludes and summarizes this dissertation.

CHAPTER 2

MODELLING ACOUSTIC PRESSURE RESPONSE

2.1 Introduction

This chapter discusses some of the modelling techniques and errors associated with characterizing acoustic pressure response. Traditional modelling techniques will be related to modal analysis methods. The latter has received increased interest recently because of the advancement of microcomputers and implementation of the Fast Fourier Transform.

2.2 Boundary Conditions of Real Volumes

The acoustic pressure response of an enclosed volume is an interaction between the properties of the volume and the acoustic excitation. The volume properties are those which describe the medium and the boundary conditions. The properties describing excitation are location, frequency, and amplitude. Most of these can be determined quite easily. Boundary conditions of real systems are often very complicated, however. They are difficult to determine quantitatively and may also have a complex geometry. Only the quantitative description will be addressed here.

At one extreme, a boundary condition may be completely absorptive, resulting in a propagating wave response. All of the acoustic pressure is absorbed at the boundary. An anechoic room is such an example. [3,4,5] The other extreme is a completely reflective boundary condition, as in a reverberant room. This results in a standing wave response.

In most real systems, these two ideal conditions are found in some combination. This is a mixed boundary condition. The resultant response should also be a combination of the propagating and standing wave responses. This has been reported experimentally [6] and analytically [7,8] when investigating acoustic intensity [9,10,11] in enclosed volumes that have boundary conditions of varying absorptivity.

The reverberant (standing wave) part of the total sound field does not contribute to the net acoustic energy flow in the room. Energy is exchanged back and forth with the sound source. [12] The direct (propagating) part of the total sound field does contribute to the energy flux.

2.3 Modelling Boundary Conditions

Predictions of the acoustic pressure response in an enclosed volume using simulations involving the wave equation [13] are straight forward. The exact value for a boundary condition is difficult to determine, however. It is generally assumed to be one of the two ideal extremes [14] for convenience. More precise characterizations of the boundary materials is possible through empirical measurement. [15-20] The standard standing wave tube technique requires measurements at discrete frequencies, a tedius and time-consuming process. If boundaries consist of several different materials, even more testing is required.

Finite element methods [21,22] have been used to predict the acoustic response of an enclosed volume. This is an especially useful method when a complex boundary is involved. But aside from the geometry, the problem of specifying the boundary condition is also encountered.

Modal analysis techniques [23,24] have been applied to acoustic systems. Systems selected for experimental comparison have been hard surfaced [25,26], with a reflective boundary condition. This is not typical in many important real acoustic systems encountered.

All of these modelling techniques are difficult to implement accurately because the boundary conditions must be estimated. At high frequencies, an assumption of an absorptive boundary condition is probably justified, because of the predominant propagating response. At low frequencies, a reflective boundary condition could be assumed, because of the predominant standing wave response. Yet, most nontrivial acoustic problems in the audible range occur in the frequency region between these extremes.

Modelling the boundary condition inaccurately can lead to significant errors in the predicted total response compared to that measured in the real system. These errors may appear small at any particular frequency when a logarithmic scale is used, but can be quite large. Optimal design of sound sources and the enclosed volumes they excite requires accurate predictions.

2.4 Predicting Response Without Boundary Information

This dissertation addresses the more likely intermediate case between the two extremes just noted. It is desirable to predict the acoustic response without requiring knowledge of the boundary condition.

A measurement based model can do this because information about the boundary condition is implicit in the empirical data. Thus, system responses can be solved directly without independent knowledge of the particular boundary condition.

This principle is used in structural modal analysis to extract natural frequencies and mode shapes from measurements of total system response. The same will be done for the acoustic system discussed here, except that a propagating wave is also extracted. The propagating wave contribution depends on the amount of boundary absorptivity.

Two-channel spectral analyzers are now readily available. Thus, simulations involving spectral analysis can be applied easily to experimental testing. There may be better formulations or microphone arrangements than the one to be presented. However, the technique which will be developed corresponds well with current equipment available to implement it.

The following chapters will develop two independent models to decompose a mixed response into propagating and standing wave components. (Figure 1) The first model will be referred to as the Analytical method. It is a one-dimensional acoustic pressure response model that requires the boundary condition to be specified. The acoustic pressure obtained will be decomposed into a propagating and a standing wave components.

The second model is the STRIPS method, which does not require knowledge of the boundary condition. The STRIPS method is a two-point spectral analysis model. Total mixed response, that may be modelled from the Analytical method or from an experiment, is input to the STRIPS method. The propagating and standing wave components obtained are compared to those obtained from the Analytical method. This matchup also allows an unknown system boundary condition to be determined.

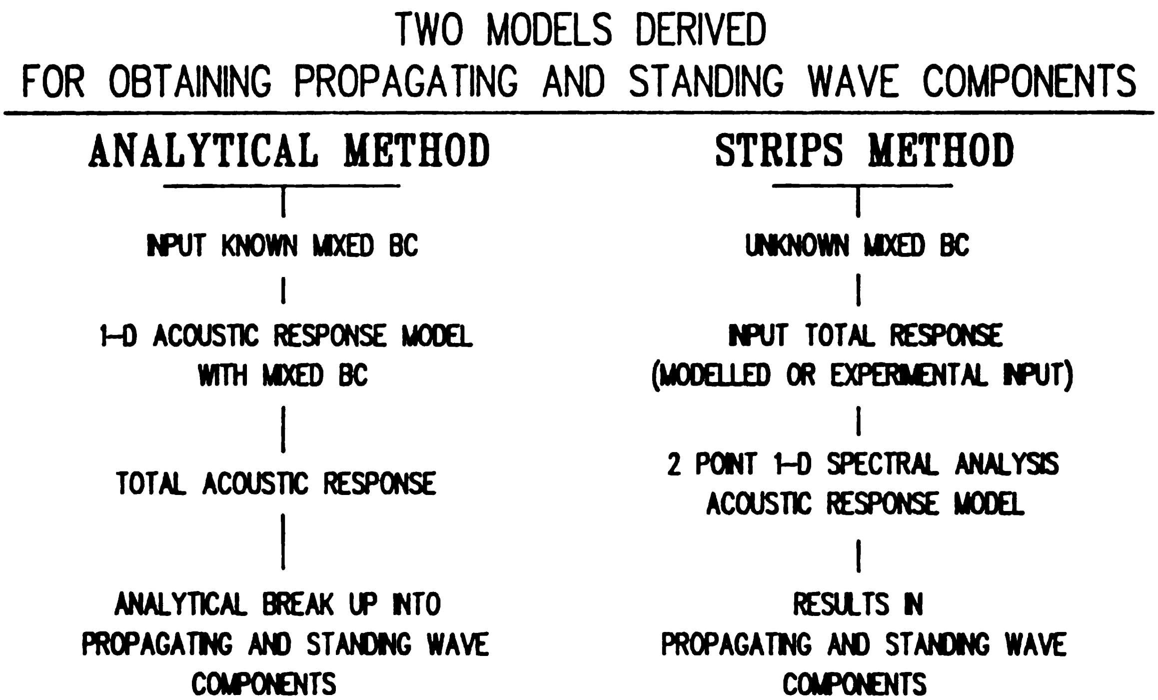

Two Models for Obtaining Components
FIGURE 1

CHAPTER 3

ANALYTICAL METHOD COMPONENTS

3.1 Acoustic Response and Boundary Conditions

A one-dimensional acoustic pressure response model will be developed to predict responses due to various specified boundary conditions. The model is useful because it corresponds to real boundary conditions, here assumed to be known. A harmonic excitation will be applied at one end.

Analytically ideal propagating and standing wave acoustic pressure responses, associated with either an absorptive or a reflective boundary condition respectively, are developed. Each pure response can be physically approximated, but neither is commonly found in the real world.

The response associated with a mixed boundary condition - one that is only partially absorptive - is also developed. It more closely approximates realistic boundary conditions. This mixed response will be equated to a summation of purely propagating and standing wave responses. These component responses are scaled and phase shifted by constants, so that they sum to form the mixed response. All three types of models and boundary conditions will be satisfied simultaneously.

Scaling factors and phase angles indicate the portions of purely propagating and standing wave response components necessary to form the total mixed response.

3.2 Reflective Boundary Condition

The one-dimensional system to be modelled can be visualized as a tube of length L. (Figure 2) In the absence of sound, the gas is assumed to have uniform density, ρ, pressure, p, and temperature, T and is at rest. It is also assumed to be non-viscous and to have zero heat conductivity, so that the only energy involved in the acoustic motion is mechanical. [27-33] The only forces are those of compressive elasticity.

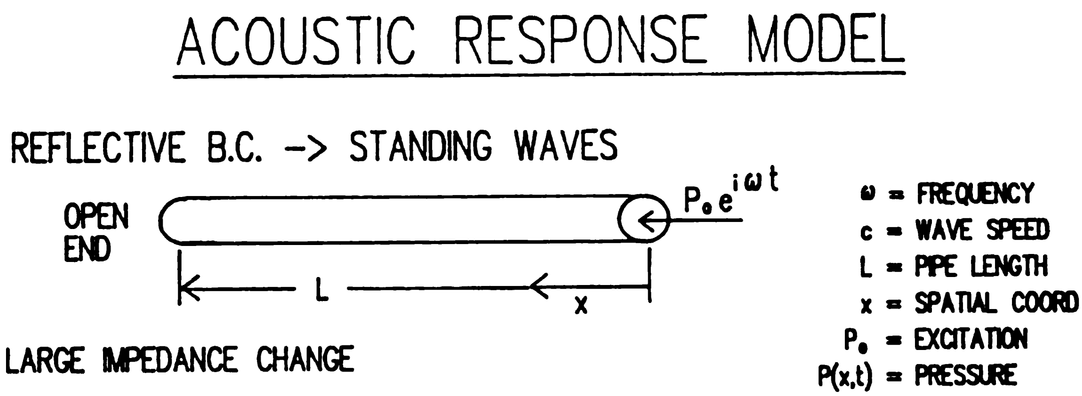

$$P(x,t) = P_0 \frac{\sin\frac{\omega}{c}(L-x)}{\sin\frac{\omega}{c}L} e^{i\omega t}$$

Standing Wave Model
FIGURE 2

The first-order equation of motion is obtained by neglecting higher-order terms and by requiring only small motions. The particle displacement, u, the wave speed, c, the time, t, and the spatial location, x, are used to formulate the wave equation in Equation 3.1.

$$\frac{\partial^2 u(x,t)}{\partial t^2} = c^2 \frac{\partial^2 u(x,t)}{\partial x^2} \tag{3.1}$$

Implicit in the wave equation is the assumption that a pressure gradient produces an acceleration of the gas and a velocity gradient produces a compression of the gas.

A harmonic [34] pressure excitation, with magnitude P_o, at location $x = 0$ is represented by the boundary condition in Equation 3.2.

$$-\rho c^2 S \frac{\partial u(0,t)}{\partial x} = P_0 S e^{i\omega t} \tag{3.2}$$

The cross-sectional area, S, has been used here. The other open end of the tube has a pressure equivalent to the ambient pressure, as in Equation 3.3.

$$\frac{\partial u(L,t)}{\partial x} = 0 \tag{3.3}$$

This is a reflective boundary condition because there exists a large step change in impedance at the tube opening.[35]

Equation 3.1 is solved by separation of variables [36-39] to obtain the particle displacement, u. Acoustic pressure is related to the spatial gradient of the particle displacement, or strain, by Equation 3.4.

$$P(x,t) = -\rho c^2 \frac{\partial u}{\partial x} \tag{3.4}$$

The linear one-dimensional steady state acoustic pressure response is shown in Equation 3.5.

$$P(x,t) = P_o \frac{\sin\left[\frac{\omega}{c}(L-x)\right]}{\sin(\frac{\omega}{c}L)} e^{i\omega t} \tag{3.5}$$

It has a sinusoidal magnitude distribution that is either in-phase or out-of-phase with respect to the excitation, as in Figure 3.

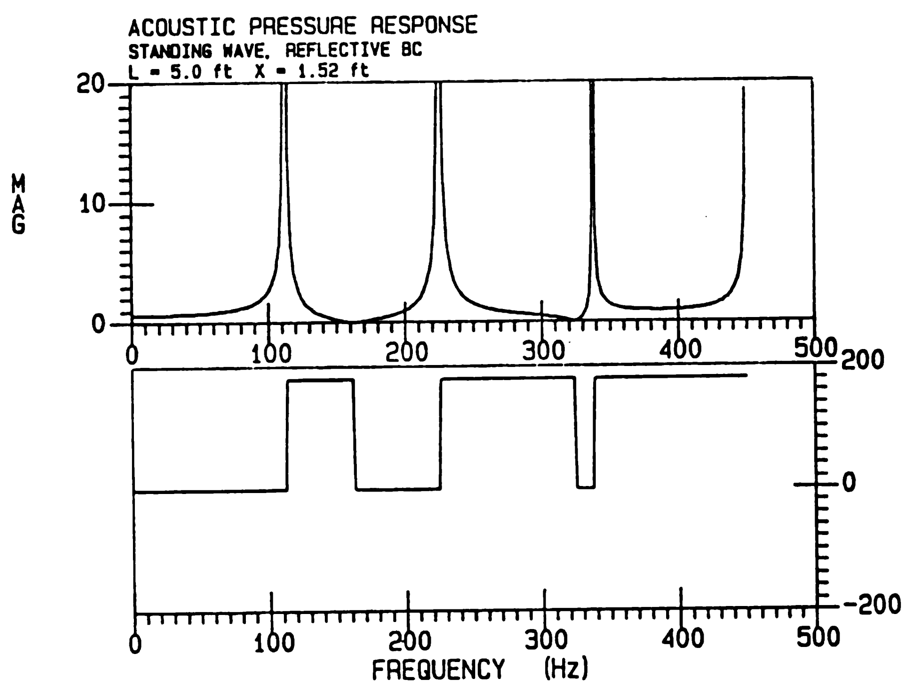

Standing Wave Response
FIGURE 3

Since no internal damping has been assumed, the ideal standing wave response resulting from a reflective boundary condition is infinite at a natural frequency, ω_n, in Equation 3.6.

$$\omega_n = \frac{n\pi c}{L} \quad , \; n = 0,1,2,3... \tag{3.6}$$

These natural frequencies, or eigenvalues, each have an associated mode shape, or eigenfunction in Equation 3.7.

$$\sin\left[\frac{n\pi}{L}(L-x)\right] \quad , \; n = 0,1,2,3,... \tag{3.7}$$

An impedance match exists with the excitation at the natural frequencies, ω_n.

3.3 Absorptive Boundary Condition

An absorptive boundary condition is modelled, Equation 3.8, by a viscous dissipation (Figure 4) placed at the tube opening, which absorbs all the acoustic pressure there.

$$-\rho c^2 S\frac{\partial u}{\partial x}(L,t) = \rho c S\frac{\partial u}{\partial t}(L,t) \tag{3.8}$$

The harmonic excitation is modelled as before in Equation 3.2. Because no acoustic pressure is reflected from the end, a propagating wave response results in Equation 3.9.

$$P(x,t) = P_o \; e^{-i(\frac{\omega}{c}x)} \; e^{i\omega t} \tag{3.9}$$

ACOUSTIC RESPONSE MODEL

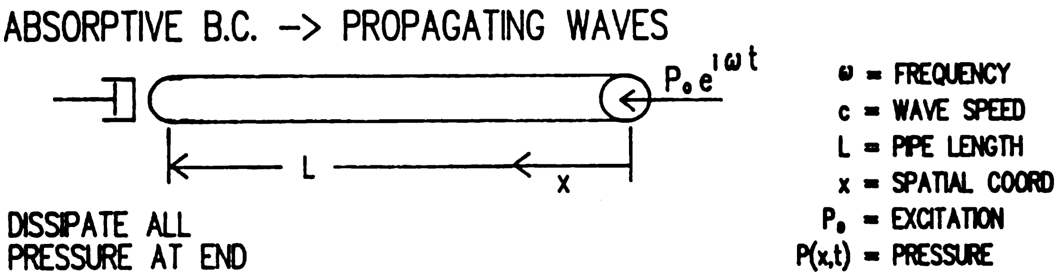

$$P(x,t) = P_o \; e^{-i\frac{\omega}{c}x} \quad e^{i\omega t}$$

Propagating Wave Model
FIGURE 4

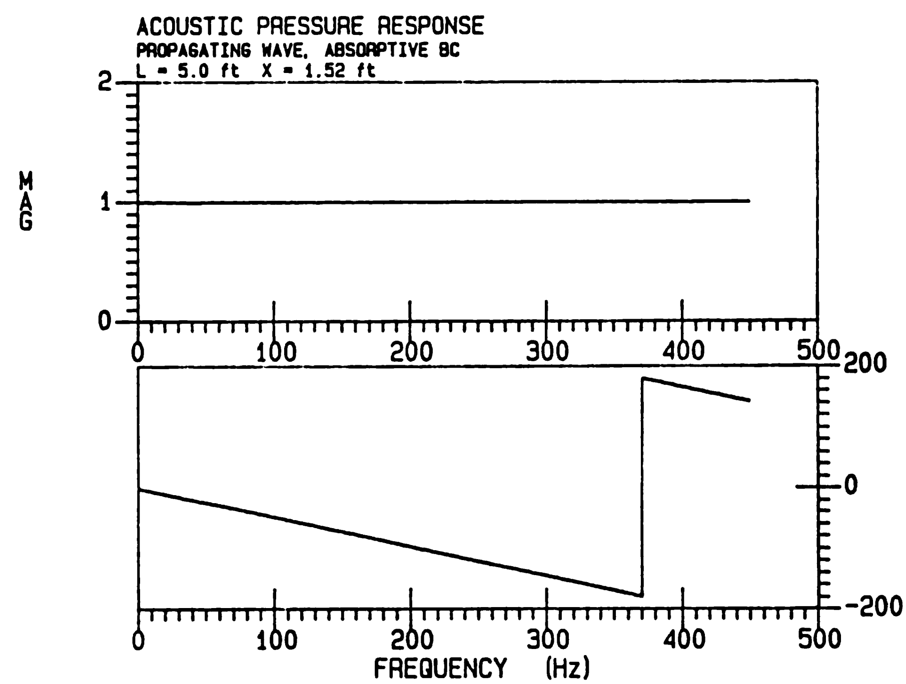

Propagating Wave Response
FIGURE 5

The excitation amplitude propagates down the length of the tube. The phase with respect to the excitation is dependent on the spatial location, or the frequency in Figure 5.

3.4 Mixed Boundary Condition

A mixed boundary condition is defined here as one which is only partially absorptive. It is modelled, Equation 3.10, again by a viscous damper at the tube end. (Figure 6) However, only a fraction, 0 < K < 1, of the pressure reaching the end is dissipated.

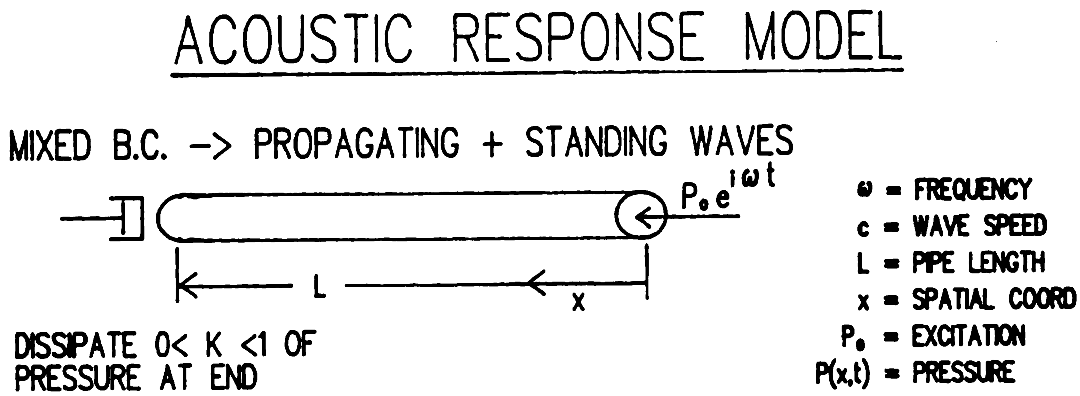

$$P(x,t) = P_0 \left[\frac{(-1+K)e^{i\frac{\omega}{c}(x-L)} + (1+K)e^{-i\frac{\omega}{c}(x-L)}}{(-1+K)e^{-i\frac{\omega}{c}L} + (1+K)e^{i\frac{\omega}{c}L}} \right] e^{i\omega t}$$

Mixed Propagating and Standing Wave Model
FIGURE 6

$$-\rho c^2 S \frac{\partial u}{\partial x}(L,t) = K \rho c S \frac{\partial u}{\partial t}(L,t) \tag{3.10}$$

The resulting mixed response, Equation 3.11, has a much more complex nature, with both real and imaginary parts.

$$P(x,t) = P_o \frac{(-1+K)e^{i\frac{\omega}{c}(x-L)} + (1+K)e^{-i\frac{\omega}{c}(x-L)}}{(-1+K)e^{-i\frac{\omega}{c}L} + (1+K)e^{i\frac{\omega}{c}L}} e^{i\omega t} \tag{3.11}$$

It is seen that for K = 1 in Equation 3.11, a propagating response is obtained and that for K = 0, a standing wave response is obtained. Intermediate values of K result in a mixed response.

Because the boundary condition is a combination of absorptive and reflective conditions, the response should also be a combination of propagating and standing wave responses. This is not immediately evident from Equation 3.11. The strong characteristics of an ideal standing wave response are seen in the mixed response in Figure 7, for a boundary absorptivity of K = 0.2. A stronger ideal propagating wave characteristic is seen when the boundary absorptivity is increased to K = 0.6 in Figure 8.

3.5 Equating Responses

The total mixed response is decomposed by equating it to the summation of the generalized propagating and standing wave response components in Equation 3.12. These are all normalized by the excitation, so that the final results are independent of the excitation.

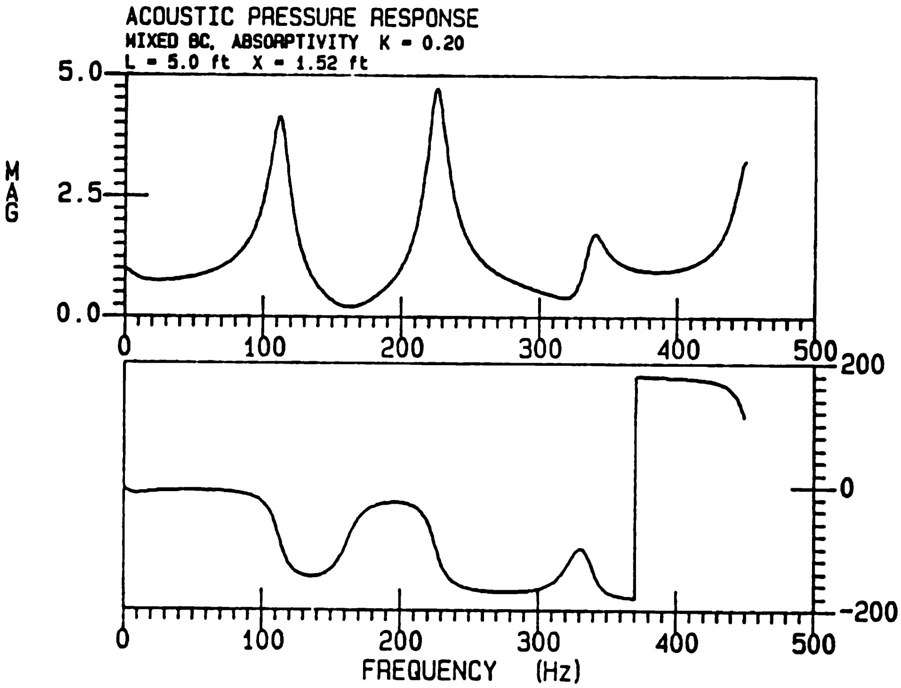

Mixed Response, K = 0.2
FIGURE 7

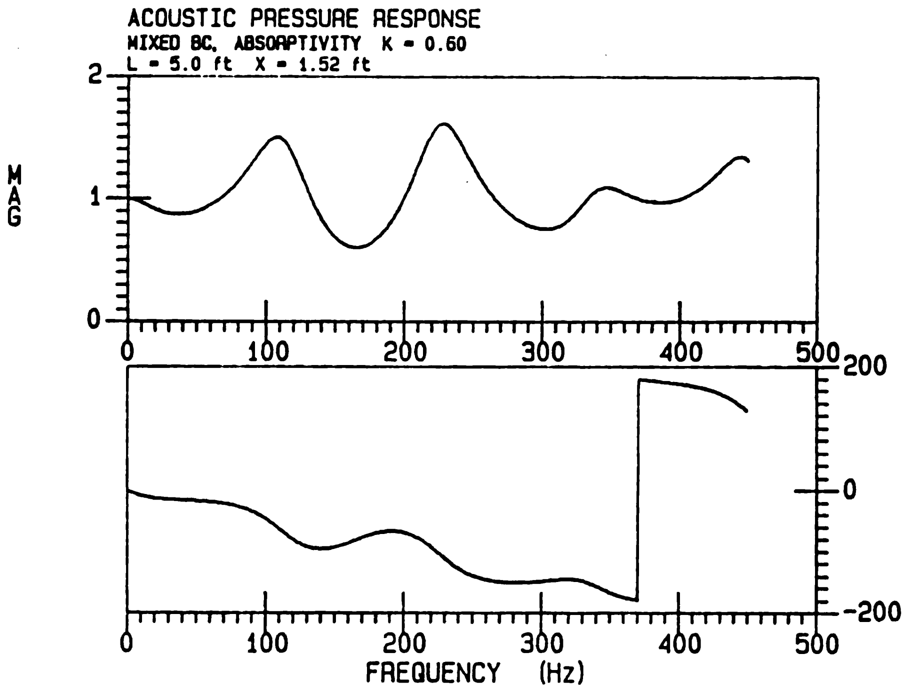

Mixed Response, K = 0.6
FIGURE 8

$$\frac{(-1+K)e^{i\frac{\omega}{c}(x-L)} + (1+K)e^{-i\frac{\omega}{c}(x-L)}}{(-1+K)e^{-i\frac{\omega}{c}L} + (1+K)e^{i\frac{\omega}{c}L}} = + A\, e^{i(\phi + \frac{\pi}{2} - \frac{\omega}{c}x)} + B\, e^{i\phi} \frac{\sin\left[\frac{\omega}{c}(L-x) + \psi\right]}{\sin(\frac{\omega}{c}L)} \tag{3.12}$$

The left-hand side of Equation 3.12 is the mixed response from Equation 3.11. The second term on the right-hand side is the standing wave response. It is multiplied by an unknown scale factor, B, and also allowed to have an unknown time phase shift, ϕ, with respect to the mixed response.

The standing wave component also requires an additional unknown spatial phase shift, ψ. The partially absorptive boundary condition causes the backward-traveling reflected wave to have a smaller magnitude than the forward-traveling wave. A standing wave results from the summation and cancellation of the two waves. However, the nodes, or points of zero response, will be at locations different from those of an ideal standing wave. Therefore, an ideal standing wave must be spatially phase shifted to correspond.

The first term on right-hand side of Equation 3.12 is the propagating component. An unknown scale factor, A, multiplies it. It is allowed an unknown temporal phase shift, ϕ, with respect to the mixed response. The phase of the propagating wave response, of course, leads the standing wave response by ninety degrees.

A and B are the scale factors for the ideal propagating and standing wave component responses contained in the mixed response. With A, B, ϕ, and ψ solved, it is possible to decompose any total mixed response into purely propagating and standing wave responses.

3.6 Analytical Method Equations

Four common factors are found when Equation 3.12 is expanded. (Appendix 2) They are; $\cos(\frac{\omega}{c}x)$, $\sin(\frac{\omega}{c}x)$, $i\cos(\frac{\omega}{c}x)$, and $i\sin(\frac{\omega}{c}x)$. The terms of Equation 3.12 multiplying $\cos(\frac{\omega}{c}x)$ are shown in Equation 3.13. Similarly the terms in Equation 3.12 multiplying $\sin(\frac{\omega}{c}x)$, $i\cos(\frac{\omega}{c}x)$, and $i\sin(\frac{\omega}{c}x)$ are shown in Equations 3.14, 3.15, and 3.16, respectively. If each equation is satisfied, the results are independent of x.

$$\begin{aligned} K\sin(\tfrac{\omega}{c}L)\cos(\tfrac{\omega}{c}L) = & -AK\sin(\tfrac{\omega}{c}L)\cos(\tfrac{\omega}{c}L)\sin\phi - A\sin^2(\tfrac{\omega}{c}L)\cos\phi \\ & -B\sin(\tfrac{\omega}{c}L)\cos\psi\left[\sin(\tfrac{\omega}{c}L)\sin\phi - K\cos(\tfrac{\omega}{c}L)\cos\phi\right] \\ & -B\cos(\tfrac{\omega}{c}L)\sin\psi\left[\sin(\tfrac{\omega}{c}L)\sin\phi - K\cos(\tfrac{\omega}{c}L)\cos\phi\right] \end{aligned} \tag{3.13}$$

$$\begin{aligned} K\sin^2(\tfrac{\omega}{c}L) = & \ AK\sin(\tfrac{\omega}{c}L)\cos(\tfrac{\omega}{c}L)\cos\phi - A\sin^2(\tfrac{\omega}{c}L)\sin\phi \\ & +B\cos(\tfrac{\omega}{c}L)\cos\psi\left[\sin(\tfrac{\omega}{c}L)\sin\phi - K\cos(\tfrac{\omega}{c}L)\cos\phi\right] \\ & -B\sin(\tfrac{\omega}{c}L)\sin\psi\left[\sin(\tfrac{\omega}{c}L)\sin\phi - K\cos(\tfrac{\omega}{c}L)\cos\phi\right] \end{aligned} \tag{3.14}$$

$$\begin{aligned} \sin^2(\tfrac{\omega}{c}L) = & \ AK\sin(\tfrac{\omega}{c}L)\cos(\tfrac{\omega}{c}L)\cos\phi - A\sin^2(\tfrac{\omega}{c}L)\sin\phi \\ & +B\sin(\tfrac{\omega}{c}L)\cos\psi\left[K\cos(\tfrac{\omega}{c}L)\sin\phi + \sin(\tfrac{\omega}{c}L)\cos\phi\right] \\ & +B\cos(\tfrac{\omega}{c}L)\sin\psi\left[K\cos(\tfrac{\omega}{c}L)\sin\phi + \sin(\tfrac{\omega}{c}L)\cos\phi\right] \end{aligned} \tag{3.15}$$

$$\begin{aligned} -\sin(\tfrac{\omega}{c}L)\cos(\tfrac{\omega}{c}L) = & \ AK\sin(\tfrac{\omega}{c}L)\cos(\tfrac{\omega}{c}L)\sin\phi + A\sin^2(\tfrac{\omega}{c}L)\cos\phi \\ & -B\cos(\tfrac{\omega}{c}L)\cos\psi\left[K\cos(\tfrac{\omega}{c}L)\sin\phi + \sin(\tfrac{\omega}{c}L)\cos\phi\right] \\ & +B\sin(\tfrac{\omega}{c}L)\sin\psi\left[K\cos(\tfrac{\omega}{c}L)\sin\phi + \sin(\tfrac{\omega}{c}L)\cos\phi\right] \end{aligned} \tag{3.16}$$

3.7 Analytical Method Solutions

These equations are solved simultaneously (Appendix 2) to obtain the exact solutions for A, B, ϕ, and ψ in Equations 3.17-3.20. A, B, ϕ, and ψ are functions of K and, of course, ω, L, and c. A is the portion of an ideal propagating wave pressure response and B is the portion of an ideal standing wave pressure response. They represent the response with an ideal absorptive or reflective boundary condition, respectively.

$$\tan\phi = \frac{-K}{(K^2-1)\sin(\frac{\omega}{c}L)\ \cos(\frac{\omega}{c}L)} \tag{3.17}$$

$$\tan(\psi-\phi) = \frac{-K}{\tan(\frac{\omega}{c}L)} \tag{3.18}$$

$$A = -\sin\phi \tag{3.19}$$

$$B = \frac{K-1}{(K-1)\cos(\psi-\phi) + \left[\tan(\frac{\omega}{c}L) + \frac{K}{\tan(\frac{\omega}{c}L)}\right]\sin(\psi-\phi)} \tag{3.20}$$

Any mixed response can be decomposed into ideal propagating and standing wave component responses, if the boundary absorptivity implied by K is specified.

3.8 Discussion of Analytical Solutions

The scale factors, A and B, are shown in Figure 9 versus frequency. The values calculated are for a boundary condition which absorbs twenty percent, K = 0.2, of the acoustic pressure at the end of a five foot, L = 5, tube. For this tube, standing wave natural frequencies, Equation 3.6, occur at an integer multiple of 112.8 Hertz.

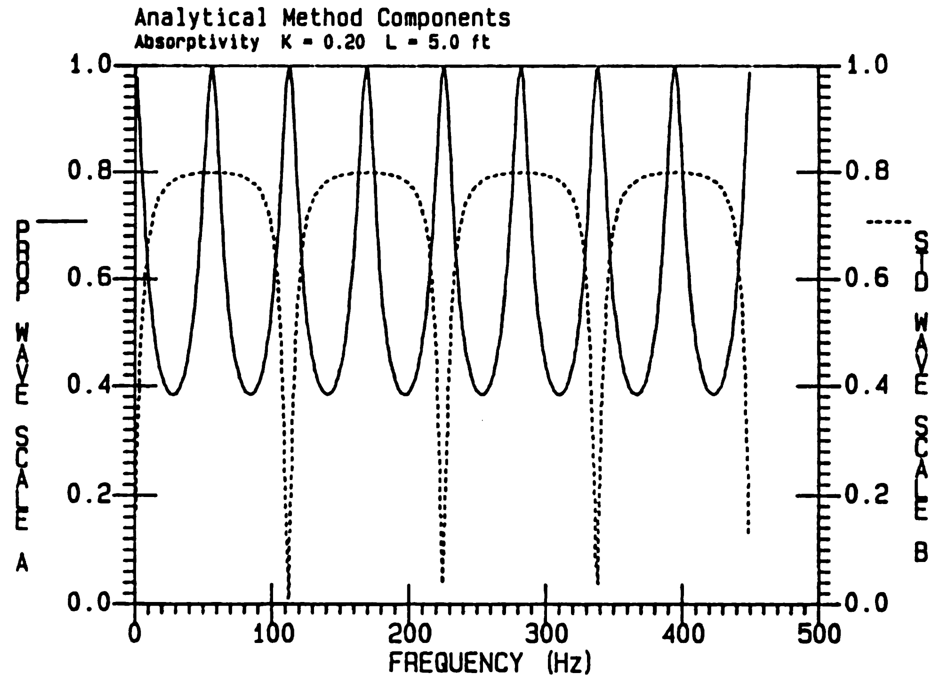

Propagating and Standing Wave Scale Factors, K = 0.2
FIGURE 9

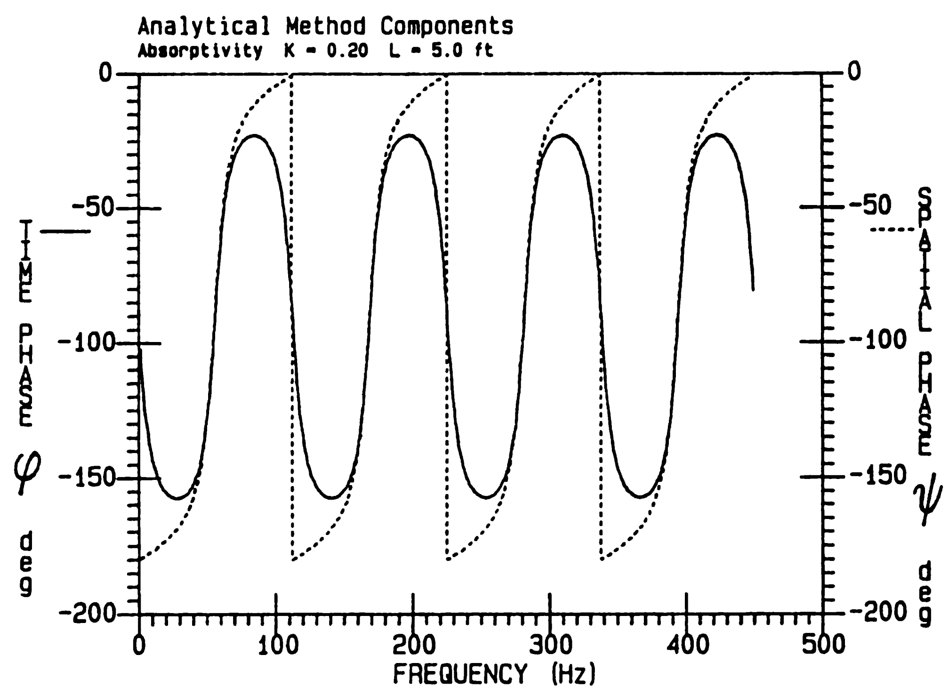

Time and Spatial Phase Angles, K = 0.2
FIGURE 10

The ideal standing wave scale factor, B, is the dotted line. The mixed response is always finite, from Equation 3.11. Therefore, B approaches zero at a natural frequency because the ideal undamped standing wave approaches infinity as the denominator in Equation 3.5 approaches zero.

At frequencies mid-way between natural frequencies, $\frac{\omega}{c}L$ is equal to ninety degrees and the ideal standing wave is not magnified by the denominator in Equation 3.5. The ideal standing wave component is (1-K), or eighty percent in this case. The other twenty percent of the pressure has been absorbed at the boundary. The boundary condition absorptivity can be determined directly from the height of the inverted B troughs. The height of the inverted B troughs will decrease as the boundary absorptivity is increased. For no boundary absorption, K = 0, B is equal to one. For K = 1, B is equal to zero.

The ideal propagating wave scale factor, A, is the solid line in Figure 9. It is unity at natural frequencies and mid-way between natural frequencies. There is an impedance match at these frequencies at the tube entrance. The height of the A troughs is proportional to the boundary absorptivity, K. The trough heights will increase as the absorption increases. For K = 1, the total response is all propagating wave response and A = 1. A is zero when K = 0.

Figure 10 shows the Analytical method time phase angle, ϕ, and the spatial phase angle, ψ, for the same boundary condition and tube length. The time phase angle, ϕ, oscillates around minus ninety degrees. It is minus ninety degrees at natural frequencies and mid-way between natural frequencies. The range of the oscillation becomes smaller as the boundary absorptivity is increased.

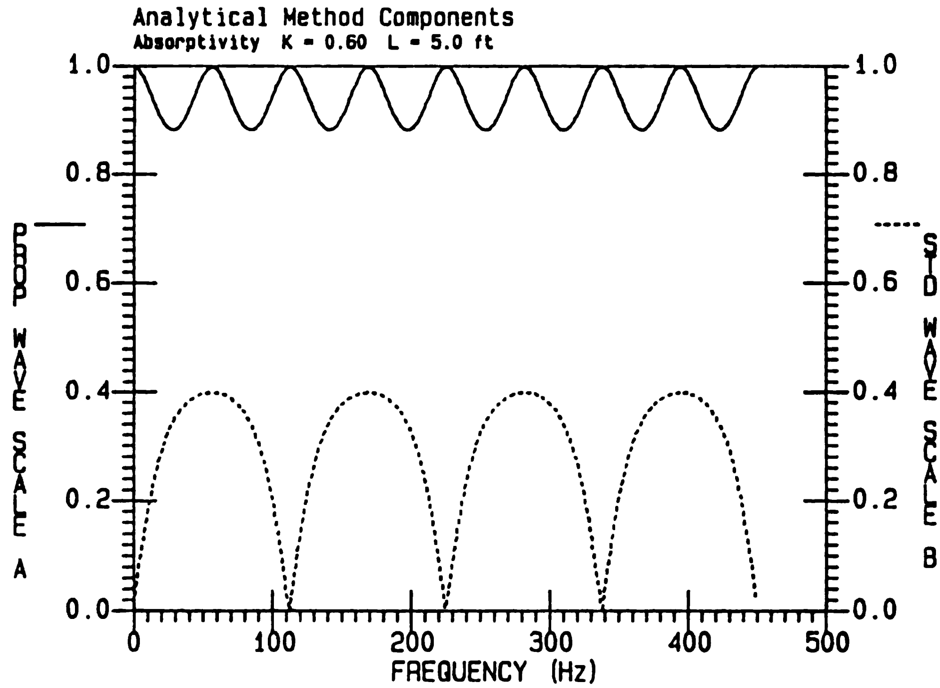

Propagating and Standing Wave Scale Factors, K = 0.6
FIGURE 11

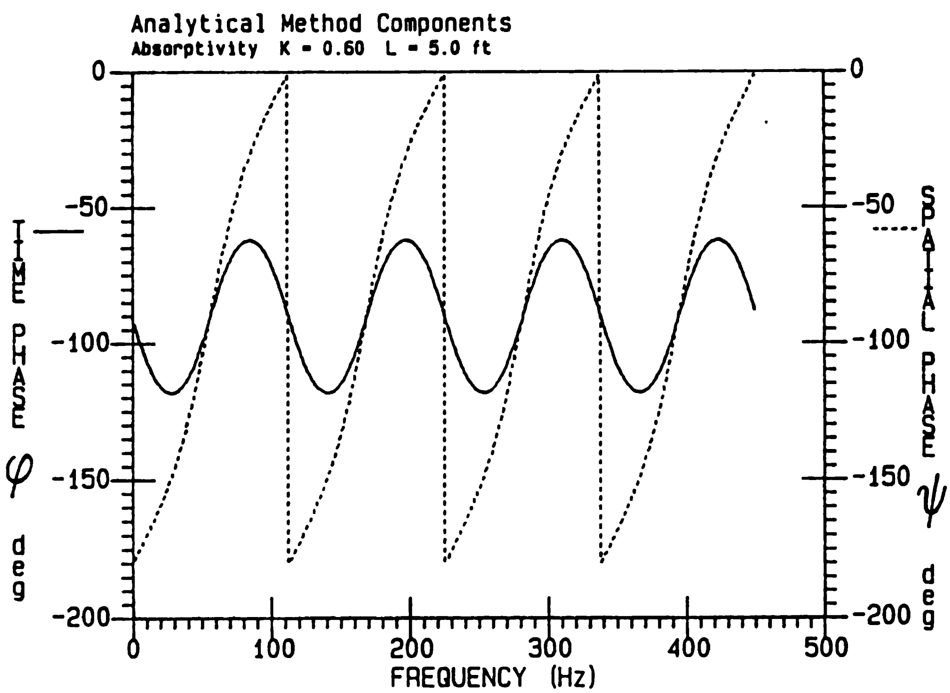

Time and Spatial Phase Angles, K = 0.6
FIGURE 12

The spatial phase angle, ψ, varies from minus one hundred eighty degrees at a natural frequency to zero degrees at the next natural frequency. It is ninety degrees different from ϕ at a natural frequency and equals ϕ mid-way between natural frequencies. The variation of ψ becomes more linear as the boundary absorbtion is increased, although the range remains the same.

Figures 11-12 show the effect of a larger boundary absorptivity, $K = 0.6$. Again, B approaches zero at natural frequencies and (1-K) mid-way between natural frequencies. The propagating wave scale factor, A, is unity at natural frequencies and mid-way between. The A troughs are higher because the boundary absorbtion is larger. The spatial phase angle, ψ, varies in a more linear way than before. The time phase angle, ϕ, has a smaller oscillation.

Combining the standing wave scale factor, B, the phase angles, ϕ and ψ, and the ideal standing wave response in Equation 3.12 results in a standing wave pressure response component, R, in Figure 13. Here, the standing wave scale factor, B, multiplies the ideal standing wave response which includes the spatial phase angle, ψ. This is the more typical frequency response that one is accustomed to seeing. It is calculated at a location, $x = 1.52$ ft, approximately one-third of the way down the five foot tube. The boundary absorptivity is twenty percent, $K = 0.2$.

The first and second modes are clearly seen at 112.8 Hertz and 225.6 Hertz. This location is nearly at a node for the third mode and shows almost zero response at that frequency. The fourth mode is just beginning and is out-of-phase with modes one and two, as expected.

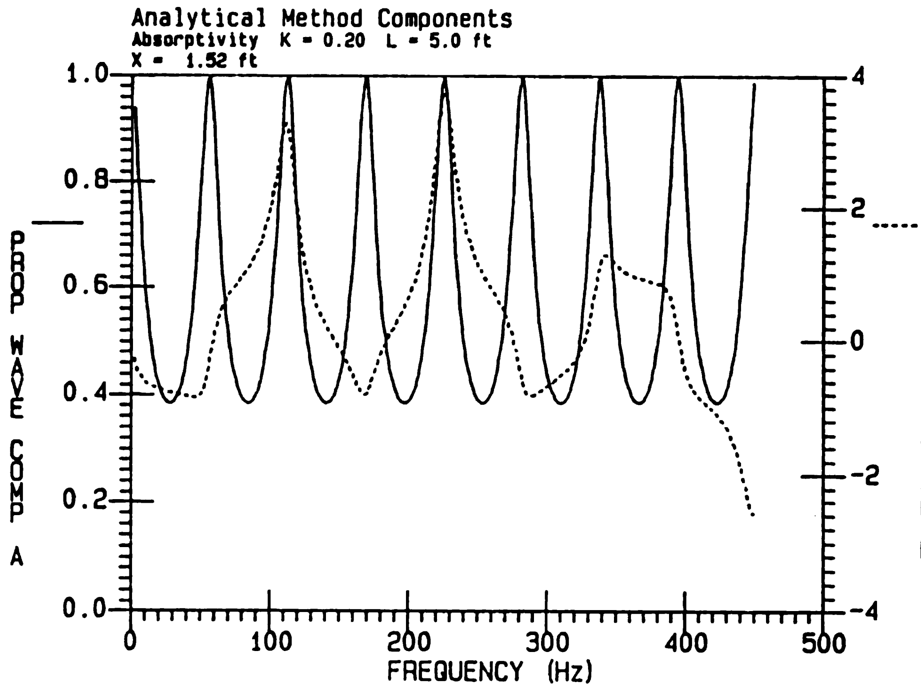

Propagating and Standing Wave Components, K = 0.2
FIGURE 13

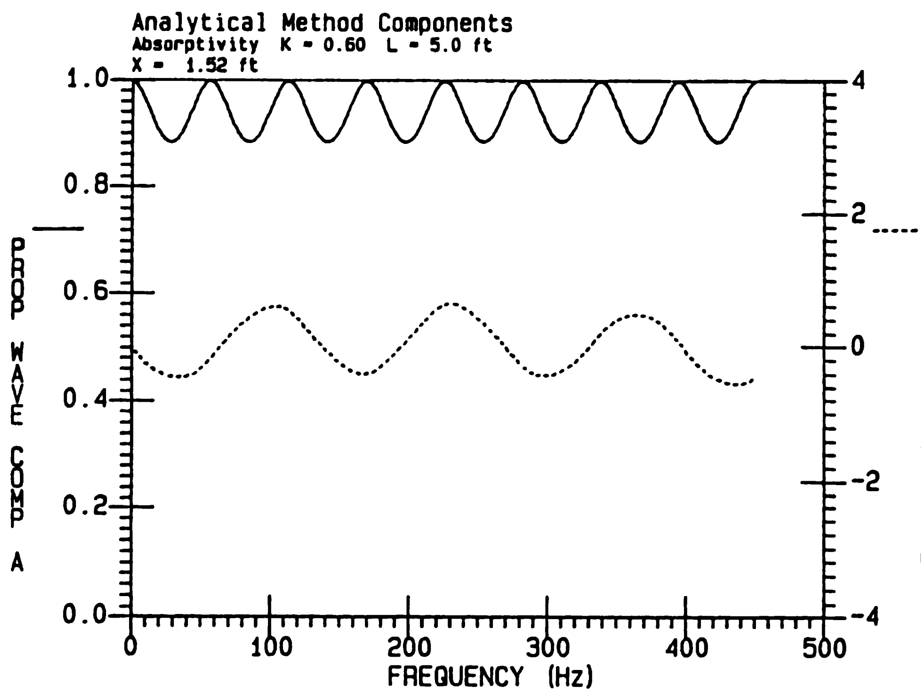

Propagating and Standing Wave Components, K = 0.6
FIGURE 14

Figure 14 shows the combined standing wave pressure component, R, for a boundary absorptivity of sixty percent, K = 0.6, at the same location. The standing wave component is much less recognizable than before because the propagating component is beginning to dominate. The modes and the node at approximately 338 Hertz are still present, however.

CHAPTER 4

STRIPS METHOD COMPONENTS

4.1 Stripping Component Response

This chapter develops the one-dimensional STRIPS method to separate total response into propagating and standing wave components. Spectral measurements of the total acoustic pressure response at two locations in a one-dimensional system are input to the STRIPS model. This total acoustic pressure response is then "stripped" into propagating and standing wave components. Closed-form STRIPS method solutions for the one-dimensional propagating wave response and the standing wave response at two measurement points are presented.

The mixed boundary condition (partially absorptive and partially reflective) does not need to be specified, as in the Analytical method. The propagating wave response component is associated with the absorptive portion of the mixed boundary condition. The standing wave response component is likewise associated with the reflective portion of the mixed boundary condition. Analyzing the propagating and standing wave response components separately is advantageous because each is associated with an ideal boundary condition. Their sum forms the total mixed response. Therefore, knowledge of the actual boundary condition is not necessary to model the total mixed response.

4.2 Propagating Wave Response

A generalized model for a one-dimensional steady state propagating wave response component, P_p, is shown in Equation 4.1. A is the unknown wave amplitude, ω is the frequency, t is the time, x is the spatial

$$P_p = A\, e^{i(\omega t - \frac{\omega}{c}x + \theta)} \tag{4.1}$$

coordinate, c is the wave velocity, and θ is the unknown initial phase angle with respect to the excitation. The spatial distribution requires that the excitation be located at x=0. At that point, the propagating wave amplitude is equal to that of the excitation.

The absolute maximum that an excitation normalized propagating response, P_p, and therefore A, can attain is unity. The phase of P_p varies linearly with x, and is equal to θ at x equal to zero. At an instant in time, the amplitude appears sinusoidal in the direction of propagation.

The propagating response leads the standing wave response by ninety degrees, so that θ in Equation 4.1 can be replaced by another unknown phase angle, ϕ, as shown in Equation 4.2.

$$P_p = A\, e^{i(\omega t - \frac{\omega}{c}x + \phi + \frac{\pi}{2})} \tag{4.2}$$

This allows a direct comparison of the phase angles in the propagating and standing wave response components.

4.3 Standing Wave Response

A general model for a one-dimensional steady state standing wave response, P_s, is shown in Equation 4.3.

$$P_s = R(x)\, e^{i(\omega t + \phi)} \tag{4.3}$$

No assumption is made of the unknown standing wave amplitude distribution, $R(x)$. It is only assumed to be a function of the spatial coordinate, x. These "mode shapes" are, of course, well known for the one-dimensional case and will be useful for comparison. They were developed in Chapter 3 for the Analytical method.

The unknown initial phase angle with respect to the excitation is given by ϕ. The standing wave phase angle lags the propagating phase by ninety degrees. All points in the standing wave response are in-phase with one another.

4.4 Total Acoustic Response

The total acoustic response, P_t, is shown in Equation 4.4 at an arbitrary location, x. It is equal to the linear summation of the propagating and standing wave response components associated with

$$P_t = P_p + P_s = A\, e^{i(\omega t - \frac{\omega}{c}x + \phi + \frac{\pi}{2})} + R(x)\, e^{i(\omega t + \phi)} \tag{4.4}$$

purely absorptive and reflective boundary conditions, as in Equations 4.2-4.3. This is the same type of decomposition of a total mixed response demonstrated by the Analytical method in Chapter 3.

At an arbitrary location, $0 < x = x_1 < L$, the total response is defined to be P_{1_t} in Equation 4.5. At another arbitrary location, $x_1 < x = x_2 < L$, the total response is defined to be P_{2_t} in Equation 4.6.

$$P_{1_t} = P_p + P_s = A\, e^{i(\omega t - \frac{\omega}{c}x_1 + \phi + \frac{\pi}{2})} + R(x_1)\, e^{i(\omega t + \phi)} \qquad (4.5)$$

$$P_{2_t} = P_p + P_s = A\, e^{i(\omega t - \frac{\omega}{c}x_2 + \phi + \frac{\pi}{2})} + R(x_2)\, e^{i(\omega t + \phi)} \qquad (4.6)$$

These are two general total mixed responses that are decomposed into propagating and standing wave components. The differences in measured magnitude and phase will be useful.

4.5 STRIPS Spectral Equations

The total response at two arbitrary points will be used to form auto-spectra and cross-spectrum. These spectral quantities can be easily measured with any of several relatively inexpensive digital Fast Fourier Transform analyzers. They can also be formed from the total response resulting from a one-dimensional acoustic response model with a specified mixed boundary condition, as in Chapter 3.

The auto-spectrum, G_{11}, of the total response at x_1 is shown in Equation 4.7.

$$G_{11} = E\{\, P^{*}_{1_t}\ P_{1_t} \,\} \qquad (4.7)$$

The E represents the expected value [40,41,43] and the * represents the complex conjugate of the quantity. The total response term is substituted from Equation 4.5 into Equation 4.7 to transform this auto-spectrum into Equation 4.8. Multiplying the terms out and then gathering similar terms finally results in Equation 4.10.

$$G_{11} = E\left\{\left[A\ e^{-i(\omega t-(\frac{\omega}{c}x_1)+\phi+\frac{\pi}{2})} + R_1\ e^{-i(\omega t+\phi)}\right] \cdot \left[A\ e^{i(\omega t-(\frac{\omega}{c}x_2)+\phi+\frac{\pi}{2})} + R_1\ e^{i(\omega t+\phi)}\right]\right\} \tag{4.8}$$

$$= E\left\{ A^2 + AR_1\ e^{-i(\frac{\pi}{2} - \frac{\omega}{c}x_1)} + AR_1\ e^{i(\frac{\pi}{2} - \frac{\omega}{c}x_2)} + R_1^2 \right\} \tag{4.9}$$

$$= E\left\{ A^2 + R_1^2 + 2AR_1\sin(\frac{\omega}{c}x_1) \right\} \tag{4.10}$$

This last equation involves the propagating wave response, A, and the standing wave response, R_1, at the point $x = x_1$.

Similarly, the auto-spectrum, G_{22}, of the total response at x_2 is shown in Equation 4.11.

$$G_{22} = E\left\{ P^*_{2_t}\ \ P_{2_t} \right\} = E\left\{ A^2 + R_2^2 + 2AR_2\sin(\frac{\omega}{c}x_2) \right\} \tag{4.11}$$

This equation also involves the propagating wave response, A, but includes the standing wave response, R_2, at the point $x = x_2$, instead.

The cross-spectrum, G_{12}, between the total responses measured at x_1 and x_2 is shown in Equation 4.12.

$$G_{12} = E\left\{ P^*_{1_t}\ \ P_{2_t} \right\} \tag{4.12}$$

The total responses from Equations 4.5-4.6 are substituted into the cross-spectrum to obtain Equation 4.13.

$$G_{12} = E\left\{\left[A\, e^{-i(\omega t-(\frac{\omega}{c}x_1)+\phi+\frac{\pi}{2})} + R_1\, e^{-i(\omega t+\phi)}\right]\right.$$
$$\left.\left[A\, e^{i(\omega t-(\frac{\omega}{c}x_2)+\phi+\frac{\pi}{2})} + R_2\, e^{i(\omega t+\phi)}\right]\right\} \tag{4.13}$$

This product is multiplied out to obtain Equation 4.14.

$$= E\left\{A^2 e^{i\frac{\omega}{c}(x_1-x_2)} + AR_2 e^{-i(\frac{\pi}{2} - \frac{\omega}{c}x_1)} + AR_1 e^{i(\frac{\pi}{2} - \frac{\omega}{c}x_2)} + R_1R_2\right\} \tag{4.14}$$

This equation is then expanded and similar terms are gathered together in Equation 4.15.

$$= E\left\{ A^2\cos\frac{\omega}{c}(x_1-x_2) + AR_1\sin(\frac{\omega}{c}x_2) + AR_2\sin(\frac{\omega}{c}x_1) + R_1R_2 \right.$$
$$\left. + i\left[A^2\sin\frac{\omega}{c}(x_1-x_2) + AR_1\cos(\frac{\omega}{c}x_2) - AR_2\cos(\frac{\omega}{c}x_1) \right] \right\} \tag{4.15}$$

4.6 STRIPS Equations

Equations 4.16-4.19 summarize the four nonlinear STRIPS equations. Auto-spectra are listed as developed before, with the expected value being understood. The cross-spectrum is divided into real and imaginary parts, $Re(G_{12})$ and $Im(G_{12})$.
Thus, four equations with three unknowns are realized.

$$G_{11} = A^2 + R_1^2 + 2AR_1\sin(\frac{\omega}{c}x_1) \tag{4.16}$$

$$G_{22} = A^2 + R_2^2 + 2AR_2\sin(\frac{\omega}{c}x_2) \tag{4.17}$$

$$Re(G_{12}) = A^2\cos\frac{\omega}{c}(x_1-x_2) + AR_1\sin(\frac{\omega}{c}x_2) + AR_2\sin(\frac{\omega}{c}x_1) + R_1R_2 \tag{4.18}$$

$$Im(G_{12}) = A^2\sin\frac{\omega}{c}(x_1-x_2) + AR_1\cos(\frac{\omega}{c}x_2) - AR_2\mathrm{Cos}(\frac{\omega}{c}x_1) \tag{4.19}$$

Simultaneous solution of the STRIPS equations results in A, R_1, and R_2. These are the propagating wave component and the standing wave components at locations x_1 and x_2.

Each of the STRIPS equations will be satisfied exactly if the unknowns, A, R_1, and R_2, are found. Other arbitrary sets of A, R_1, and R_2 will result in a residual error for each equation.

4.7 STRIPS Solutions

The STRIPS equations are solved for the propagating, A, and standing wave, R_1 and R_2, components by a least squared error analysis. (Appendix 2) This results in twelve equations with three unknowns. These are solved for the exact STRIPS solutions in Equations 4.20-4.22.

$$A = \frac{\mathrm{Im}[G_{12}]}{\left[G_{11}\cos^2(\frac{\omega}{c}x_2)+G_{22}\cos^2(\frac{\omega}{c}x_1)-2\mathrm{Re}(G_{12})\cos(\frac{\omega}{c}x_1)\cos(\frac{\omega}{c}x_2)\right]^{0.5}} \tag{4.20}$$

$$R_1 = -A\ \mathrm{Sin}(\frac{\omega}{c}x_1) \pm \left[-A^2\mathrm{Cos}(\frac{\omega}{c}x_1) + G_{11}\right]^{0.5} \tag{4.21}$$

$$R_2 = -A\ \mathrm{Sin}(\frac{\omega}{c}x_2) \pm \left[-A^2\mathrm{Cos}(\frac{\omega}{c}x_2) + G_{22}\right]^{0.5} \tag{4.22}$$

The propagating wave response component, A, is directly proportional to the imaginary part of the cross-spectrum, $\mathrm{Im}(G_{12})$. Chung's [10] cross-spectral method of measuring acoustic intensity was also proportional to the imaginary part of the cross-spectrum. Unlike the cross-spectral method, however, the denominator in the STRIPS method contains information on magnitude and phase at the two measurement points.

4.8 STRIPS Constraint and Conditions

There are four combinations of plus-minus signs to select when calculating R_1 and R_2 in Equations 4.20-4.22. These will extremize the squared residual error in the STRIPS equations, Equations 4.16-4.19. The set of STRIPS solutions which makes the squared residual error equal to zero is desired. Substituting these solutions back into the STRIPS equations (Equations 4.10-4.13) yields the necessary STRIPS constraint in Equation 4.23 to find conditions which null the squared residual error. (Appendix 2)

$$G_{11}\ G_{22} = \mathrm{Im}(G_{12})^2 + \mathrm{Re}(G_{12})^2 \qquad (4.23)$$

The STRIPS constraint is always satisfied. It is used to determine the STRIPS solution conditions.

These STRIPS conditions determine the selection of the plus or minus sign in R_1, Equation 4.21, and R_2, Equation 4.22. The STRIPS conditions are four sets of inequalities stipulating the appropriate sign combinations in Equations 4.24-4.27.

STRIPS CONDITION	SIGN SELECTION Equation 4.21	Equation 4.22	
$G_{11}\cos(\frac{\omega}{c}x_2) < \mathrm{Re}(G_{12})\cos(\frac{\omega}{c}x_1)$	+	+	(4.24)
$G_{22}\cos(\frac{\omega}{c}x_1) > \mathrm{Re}(G_{12})\cos(\frac{\omega}{c}x_2)$			
$G_{11}\cos(\frac{\omega}{c}x_2) < \mathrm{Re}(G_{12})\cos(\frac{\omega}{c}x_1)$	+	-	(4.25)
$G_{22}\cos(\frac{\omega}{c}x_1) < \mathrm{Re}(G_{12})\cos(\frac{\omega}{c}x_2)$			
$G_{11}\cos(\frac{\omega}{c}x_2) > \mathrm{Re}(G_{12})\cos(\frac{\omega}{c}x_1)$	-	+	(4.26)

$$G_{22} \cos(\frac{\omega}{c}x_1) \; > \; Re(G_{12}) \cos(\frac{\omega}{c}x_2)$$

$$G_{11} \cos(\frac{\omega}{c}x_2) \; > \; Re(G_{12}) \cos(\frac{\omega}{c}x_1) \qquad - \qquad - \qquad (4.27)$$
$$G_{22} \cos(\frac{\omega}{c}x_1) \; < \; Re(G_{12}) \cos(\frac{\omega}{c}x_2)$$

The individual terms are the same in each of the above four sets of inequalities. A determination of which of the inequalities is present is all that need be done to select the signs in Equations 4.21 and 4.22.

Measured quantities include G_{11}, G_{22}, $Re(G_{12})$, $Im(G_{12})$, x_1, x_2, ω, and c. Errors in these quantities will also cause a residual error. The sum of the squares of the residual errors will be useful to identify measurement errors. (Appendix 2)

4.9 Discussion of STRIPS Solutions

A modelled mixed response in a five foot (1.524 meters) tube was determined at 1.52 feet (0.46 meters) and at 2.01 feet (0.61 meters), using Equation 3.11. The boundary absorptivity is twenty percent, ($K = 0.2$). An experimental mixed response will be discussed later.

The auto-spectra and cross-spectrum are formed using the mixed responses at the two specified locations. STRIPS method components are found using these spectra as input to the STRIPS solutions, Equations 4.20-4.22. The resultant STRIPS propagating and standing wave components, A, R_1, and R_2, are shown in Figure 15.

No measurement error is encountered because modelled mixed responses were used. The sum of the squared residual errors (SRE) is zero at all frequencies.

The standing wave response component, R_1, has first and second modes at 112.4 and 224.8 Hertz. This location, at 1.52 feet, is approximately at a node for the third mode, and has nearly zero response there. The fourth mode is just beginning to appear. The fourth mode is out-of-phase with the first two, as it should be.

The propagating wave response component, A, is maximized at natural frequencies and mid-way between natural frequencies. It is minimized at one-quarter and three-quarter between natural frequencies.

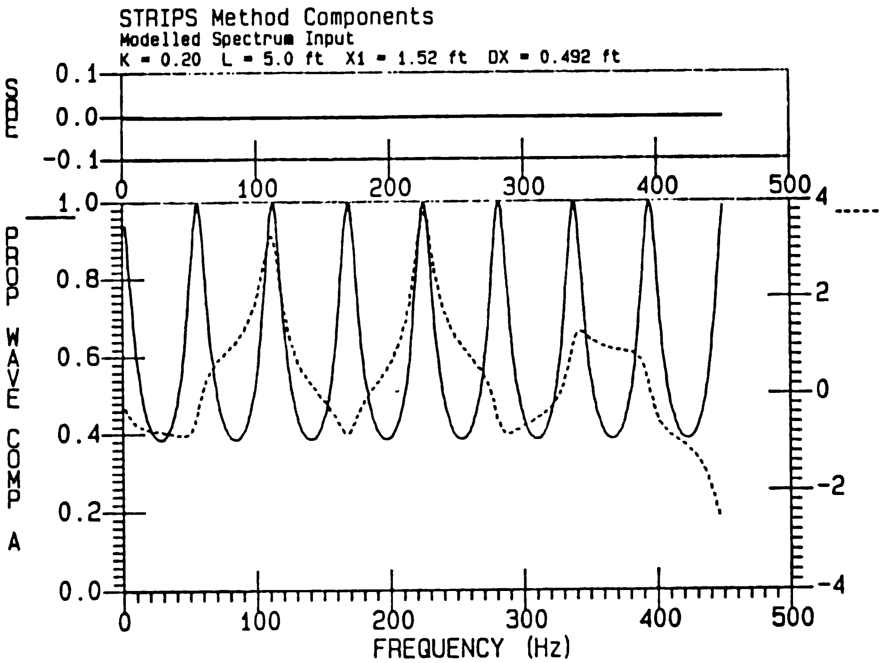

STRIPS Components, K = 0.2
FIGURE 15

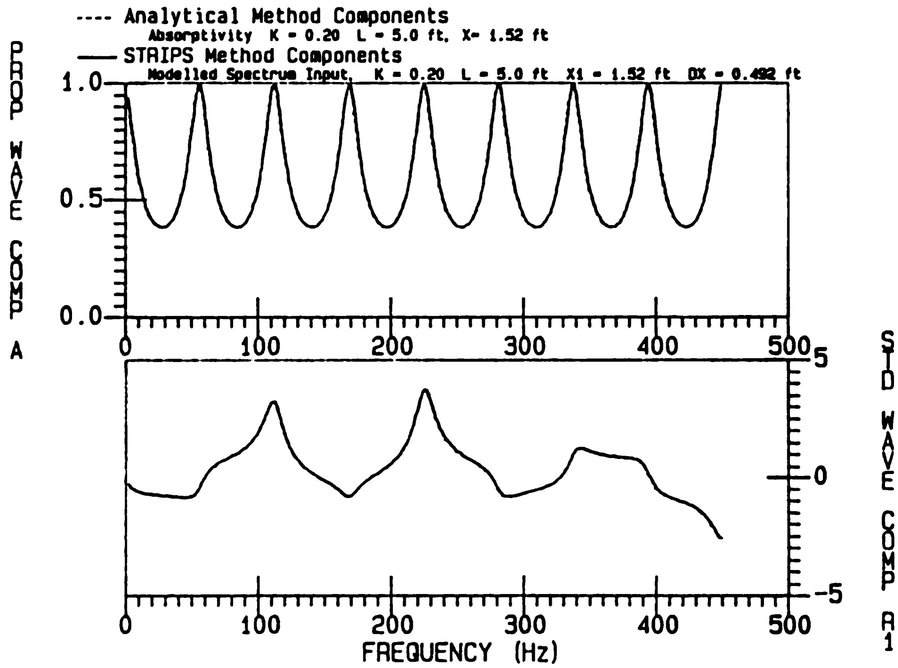

Analytical and STRIPS Comparison, K = 0.2
FIGURE 16

These STRIPS method components are compared to the Analytical method components in Figure 16. Both have the same mixed response input. They compare very well. There is no discernable difference in the curves.

The same comparison is made for a boundary absorptivity of sixty percent, K = 0.6, in Figure 17. Again, the comparison is very good. Propagating and standing wave components can be found from the total mixed response even if the the boundary condition is unknown.

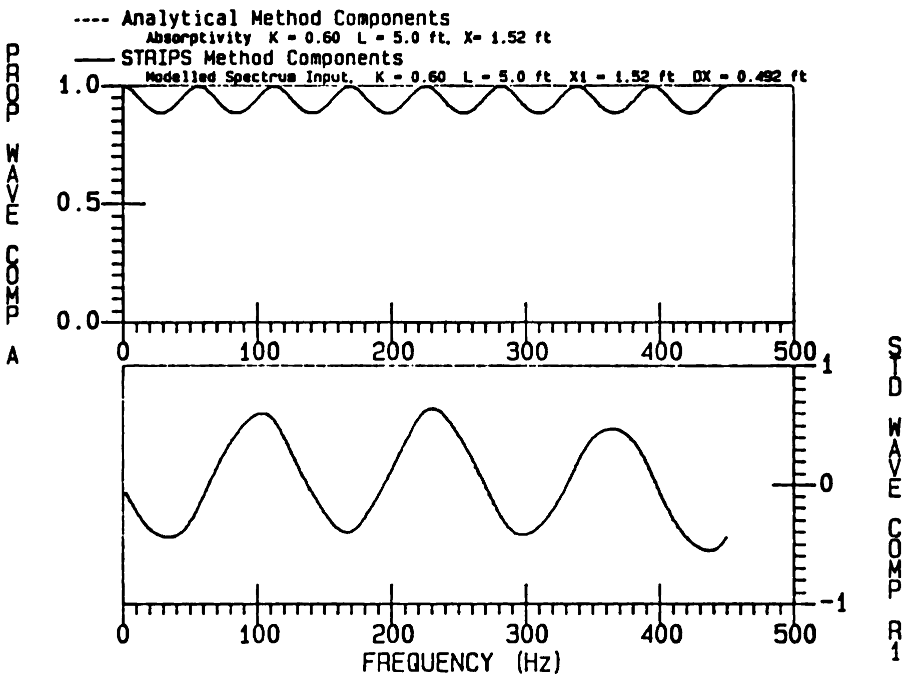

Analytical and STRIPS Comparison, K = 0.6
FIGURE 17

CHAPTER 5

EXPERIMENT

5.1 Introduction

This chapter describes the setup and tests done to obtain experimental data to allow a comparison with the analytical results previously developed. The auto-spectra and cross-spectrum of the total acoustic response at two points in a tube are input to the STRIPS method of measuring propagating and standing wave components. The tube is excited at one end with random noise. Two boundary conditions are tested at the other end. The propagating and standing wave components are then used to determine the boundary absorptivity.

5.2 Experimental Procedure

A five foot (1.524 meter) long, three inch (76.2 millimeter) inside diameter PVC pipe was used to simulate the one-dimensional plane-wave acoustic response models described in Chapter 3. Holes were drilled through one surface of the pipe at a spacing of 0.492 feet (150 millimeter), as shown in Figure 18. A two-microphone probe assembly was inserted into two holes to measure two total acoustic pressure responses. The remaining holes were plugged during the measurement. (Figure 19)

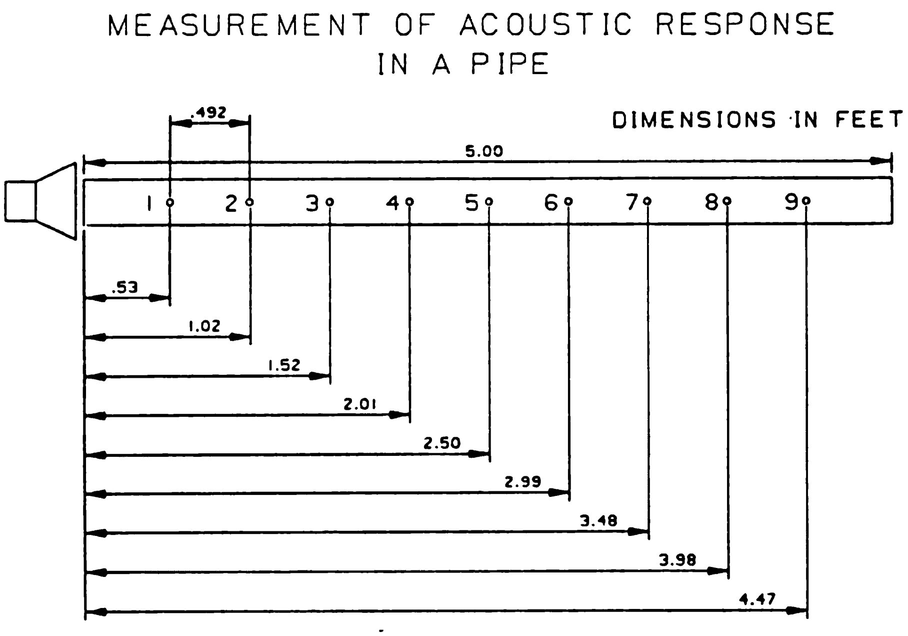

Experimental Setup Layout
FIGURE 18

Each of the one-half inch microphones (Bruel & Kjaer 4166 random incidence condenser) were calibrated with a sound level calibrator (B&K 4230). The calibrated pressure signals were connected through a microphone preamplifier (B&K 2619) to a spectral analyzer (Hewlett Packard 5423A). The analyzer also provided the band-limited (50-450 Hz) random noise signal to drive the speaker exciting the pipe entrance. The excitation was measured and used to normalize the total acoustic pressure spectra, so that the STRIPS results are independent of the excitation used.

The auto-spectra of each pressure response and the cross-spectrum between the two pressure responses were measured by the analyzer and stored on cassette tape. An ICS Electronics Corporation Model 4885A RS-232 to IEEE 488 Controller interfaced the HP analyzer to a Prime 750 mini-computer in the A.H. Case Center for Computer-Aided Design at Michigan State University. The spectra were transferred to the Prime 750 where software implementing the STRIPS method and numerous graphics capabilities reside.

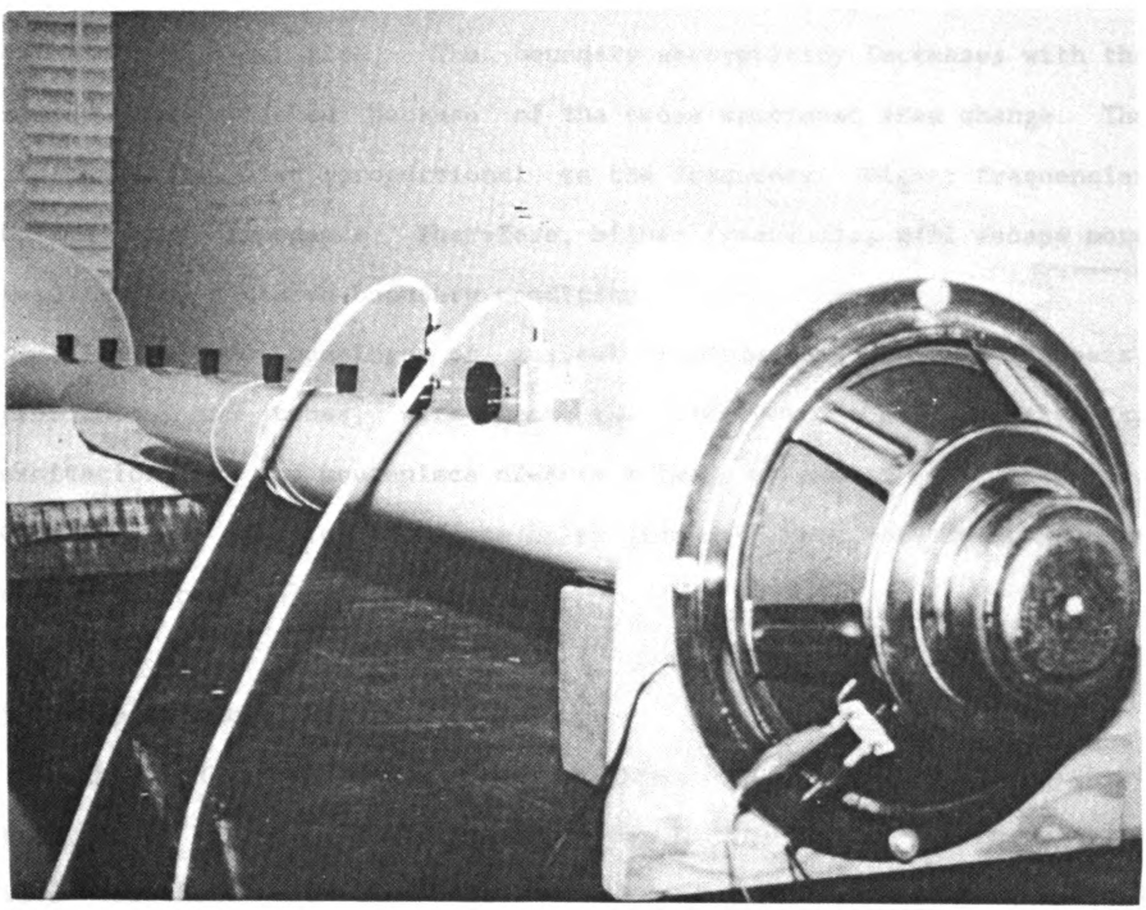

Experimental Tube Apparatus
FIGURE 19

5.3 Boundary Conditions

One boundary condition tested was an open ended configuration, simulating a nearly reflective boundary condition. The very large impedance change at the pipe end acts as an acoustic barrier. Because some acoustic energy does escape from the end of the pipe, a small absorptivity is expected.

The other boundary condition employed a flare-ended configuration in an attempt to match the impedance at the pipe end with the room impedance. Impedance is inversely proportional to the cross-sectional area. A linearly increasing flare helps to match the finite impedance inside the pipe to the essentially infinite impedance in the room exterior to the pipe. The boundary absorptivity increases with the flared end attached because of the cross-sectional area change. The impedance is also proportional to the frequency. Higher frequencies have a larger impedance. Therefore, higher frequencies will escape more readily with a flared boundary condition.

The flared openings of musical instruments, such as trumpets, trombones, and tubas, work much the same way. A relatively easy excitation at the mouthpiece creates a large output at the flared end. Changing the shape of the flare helps give different instruments higher or lower tonal qualities.

5.4 Experimental Results

The STRIPS method components at point three, x = 1.52 feet,without the flared boundary condition are shown in Figure 20. The propagating wave component has the same character of peaks and troughs predicted analytically. The frequency resolution (1.56 Hz) obtained for the bandwidth shown is not as high as that which is possible from the

Analytical model. Therefore, the propagating wave peaks do not rise all the way to unity as they should.

The heights of the troughs give an intuitive sense of the amount of absorptivity of the boundary condition. The absorptivity appears very small. The height of the troughs increases slightly with frequency, indicating that absorptivity increases with frequency. This is expected since higher frequency waves have a better impedance match with the boundary and can be absorbed more easily.

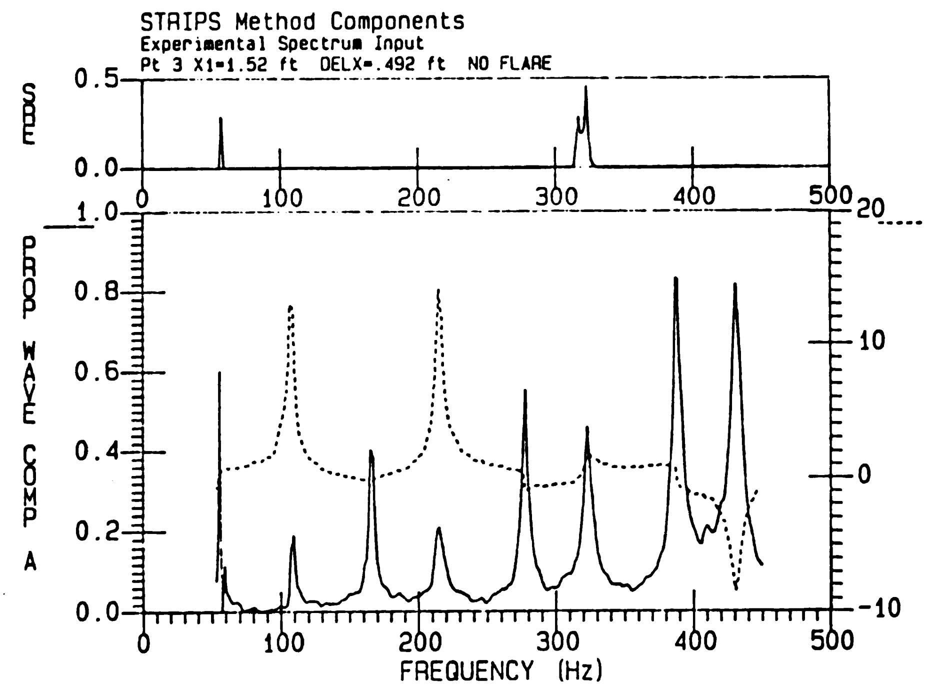

STRIPS Components, No Flared End
FIGURE 20

The standing wave component has a familiar form. The first, second, and fourth modes are evident. The third mode is nearly at a node, and has only a small response. The squared residual error (SRE) function is non-zero at points where either microphone is located at a node.

These experimental STRIPS components are compared in Figure 21 to the Analytical method components when three percent, K = 0.03, of the acoustic pressure at the pipe end is absorbed. The heights of the propagating wave troughs compare very well. The standing wave amplitudes also compare well.

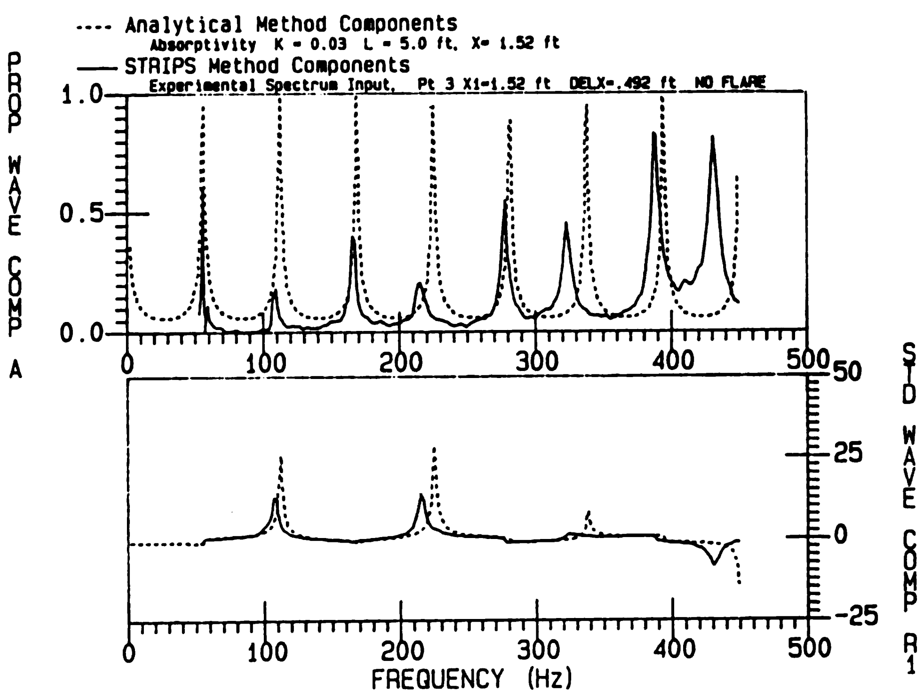

Analytical and STRIPS Comparison, K = 0.03
FIGURE 21

The modelled standing wave amplitudes are larger because no internal damping was assumed. The experimental natural frequencies become increasingly lower than the modelled natural frequencies at higher frequencies. The effective pipe length becomes longer for higher frequencies because the response waves are beginning to escape further out of the end of the pipe before being reflected back. Both of these phenomena can be used to further tune the analytical model.

The STRIPS experimental propagating wave component is very similar to that predicted by the Analytical method. It is obvious that low frequencies have less absorption and higher frequencies more absorption than the constant $K = 0.03$ shown. The change in the effective length of the pipe can again be seen by the difference in the frequencies at which the peaks occur. The experimental peaks become increasingly lower than those predicted at higher frequencies.

The STRIPS components found from experimental spectra input when the flared end was attached are shown in Figure 22. The propagating component is virtually unchanged at lower frequencies. There is more propagation at higher frequencies, however. This is expected since higher frequencies are affected more by the change in impedance at the tube end than the lower frequencies are.

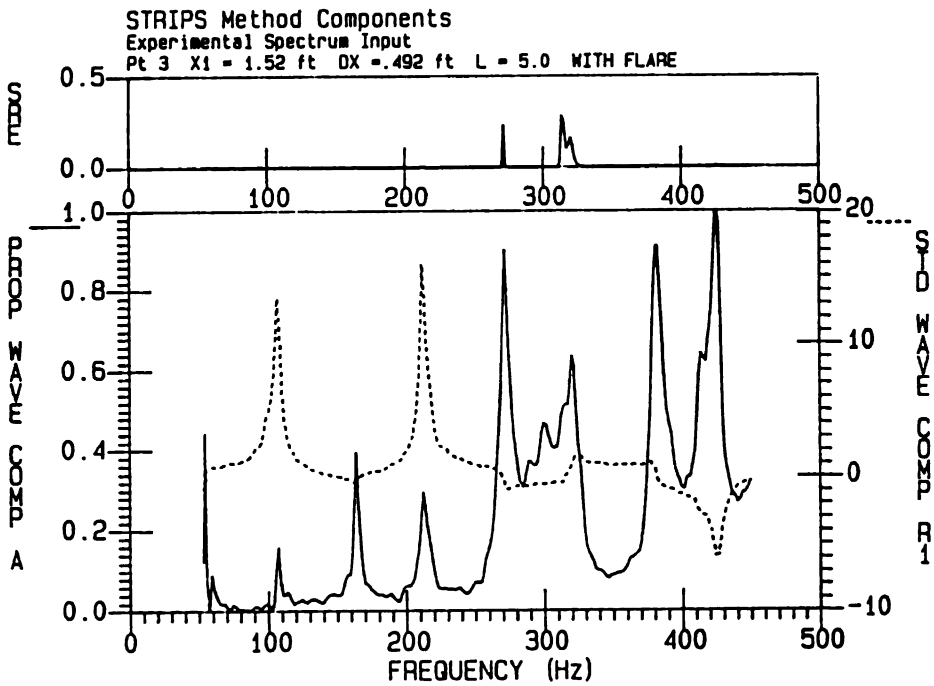

STRIPS Components, With Flared End
FIGURE 22

CHAPTER 6

CONCLUSIONS

6.1 Summary

The manner in which one views the boundary condition of an enclosed volume, and therefore its acoustic pressure response, plays an important role in selecting the model used to predict the response. An accurate description of the boundary condition is needed in order to obtain accurate predictions of the acoustic pressure response at some point in an enclosed volume. It is difficult to determine either the absorptivity or the geometry of most important systems of interest.

Few enclosed volumes have completely absorptive boundary conditions, as an anechoic room does. Most realistic boundary conditions are partially absorptive, with the rest of the acoustic pressure being reflected. This is a mixed boundary condition.

A mixed boundary condition can be considered as being composed of portions of an ideal absorptive and an ideal reflective boundary condition. Each ideal extreme has a well-known response associated with it. An absorptive boundary condition is associated with a propagating wave response. A reflective boundary condition is associated with a standing wave response.

A mixed response results from a mixed boundary condition. Since the mixed boundary condition can be decomposed into two ideal extremes, the same should be possible for the mixed response. The mixed response can be thought of being made up of a summation of propagating and standing wave responses. Each has distinguishing characteristics.

A propagating wave response measured at two points is characterized by a constant amplitude, but a changing phase with respect to the excitation. A standing wave response is characterized by a changing amplitude, but a constant phase with respect to the excitation. These characteristics are superimposed in a mixed response.

Finding these analytically ideal components directly from measurements of the mixed response is desirable because then the actual boundary condition is not needed. The characteristics of the ideal responses can be used to "strip" the two components from the total mixed response.

A one-dimensional mixed response was analytically formed using a specified mixed boundary condition. Harmonic excitation was applied to the other end. An Analytical method for decomposing the mixed response into propagating and standing wave components was developed. The results were scale factors, A and B, multiplying the ideal propagating and standing wave response components. Phase angles, ϕ and ψ, were also found to account for the time and spatial phase shift needed. They were found such that the ideal components sum to the total mixed response. All responses were normalized by the excitation, so that the maximum scale factor possible was unity.

The standing wave scale factor, B, must go to zero at natural frequencies, where the ideal standing wave response goes to infinity. The ideal standing wave is not magnified mid-way between natural frequencies. The standing wave scale factor is one minus the boundary absorptivity (1-K), there. The remainder is absorbed at the boundary. A standing wave component, R, is obtained by multiplying the scale factor, B, times the ideal standing wave and including the effect of the phase angles. The standing wave response component has the typical natural frequencies and mode shapes found in modal analysis.

The scale factor, A, multiplying the ideal propagating wave response is the magnitude of the propagating pressure wave response component. It is always unity at natural frequencies and mid-way between natural frequencies. At one-quarter and three-quarter between natural frequencies the propagating wave component is minimized. The propagating wave component there is indirectly related to the boundary absorptivity, K. The height of these troughs becomes higher as the boundary absorptivity is increased.

A STRIPS method to separate total response into propagating and standing wave response was developed. This technique is intended for application to experimental measurements of acoustic pressure response. The actual mixed boundary condition is not known in this case.

STRIPS is a two-point spectral analysis model which includes measurements of the total mixed response. The results are the propagating and standing wave response components, A, R_1, and R_2. They were found to compare very well with the Analytical method components mentioned above in both the simulation and laboratory tests. Including effects of wall interactions, internal damping, end effects, and the change in effective tube length will increase the utility of the predictions.

A STRIPS squared error function also results from the STRIPS method. It is zero if the system from which the measured responses are taken from fit the derived model. System deviations from this model will result in a STRIPS squared error. A person using the STRIPS method on a microcomputer could use the STRIPS error as an indicator of whether good results were obtained. Knowledge of the details the analysis would not be needed. In laboratory tests, an error was seen when one of the microphones was at a standing wave node of the tube tested. The STRIPS error was zero at other frequencies, showing that the real system matched the model well.

The microphone spacing must be wide enough so that information on both the magnitude change of the standing wave and the phase change of the propagating wave is measured. A topic for future investigation is the minimum and maximum frequency that can be measured for a specified microphone spacing. A maximum frequency should be realized when multiple standing wave nodes exist between the microphones.

A one-dimensional modal analysis is possible from the "stripped" standing wave response component. Natural frequencies and mode shapes can be extracted. The portion of standing wave response present is dependent on the amount of absorptivity at the boundary. Another future topic is to develop the method to increase accuracy of three-dimensional modal analysis. This topic is of more general interest, but must be approached carefully because of symetry problems.

The boundary condition, at first unknown, can be found by matching the STRIPS components to the Analytical components, which are a function of the boundary absorptivity. This defines the active part of the impedance at the boundary. A more general case is to represent the boundary absorptivity as a general complex impedance. The potential exists to build a system in the future which measures the absorptivity of a material placed at the pipe end.

The STRIPS method of measuring propagating and standing wave components contributes a method to obtain accurate information about boundary conditions in realistic enclosures. It allows more detailed models of acoustic pressure response to be developed because the modelled boundary condition parameters are based on measurements. This research has been a first step which demonstrates the concept with a one-dimensional system. As the technique and hardware are improved, the goal is to measure a general complex boundary impedance in a three-dimensional enclosed volume. STRIPS has started the work towards this goal.

APPENDICES

APPENDIX 1

ANALYTICAL METHOD SOLUTIONS

A1.1 Ideal and Mixed Boundary Conditions

Representative one-dimensional steady state acoustic pressure responses due to a harmonic excitation and various boundary conditions were developed in Chapter 3. An absorptive boundary condition results in a propagating wave response. A reflective boundary condition results in a standing wave response. A combination of these two ideal boundary conditions results in a mixed response.

This appendix develops the Analytical Method to decompose a mixed acoustic response into the summation of ideal propagating and standing wave component responses. The mixed boundary condition is known for the Analytical method.

A1.2 Ideal and Mixed Responses

A one-dimensional plane wave acoustic pressure response associated with a mixed boundary condition was developed in Chapter 3 and is repeated in Equation A1.1. A mixed boundary condition is one that is partially absorptive and partially reflective. The mixed response in Equation A1.1 has been normalized by a general harmonic excitation.

$$\frac{(-1+K)e^{i\frac{\omega}{c}(x-L)} + (1+K)e^{-i\frac{\omega}{c}(x-L)}}{(-1+K)e^{-i\frac{\omega}{c}L} + (1+K)e^{i\frac{\omega}{c}L}} \qquad (A1.1)$$

It has a phase with respect to the excitation and magnitude that is dependant on, among other things, the boundary condition absorptivity, K, the displacement, x, and the frequency, ω.

A propagating response is shown in Equation A1.2. It has also been normalized by the excitation. It is multiplied by an unknown scaling factor, A, and has an unknown phase angle, ϕ, with respect to the mixed response.

$$A\ e^{i(\phi + \frac{\pi}{2} - \frac{\omega}{c}x)} \qquad (A1.2)$$

The scale factor, A, represents the portion of a ideal propagating wave response.

A standing wave response in Equation A1.3 has also been normalized by the excitation. Its unknown scaling factor, B, is multiplying a sinusoidally varying spatial distribution.

$$B\ e^{i\phi}\ \frac{\sin[\frac{\omega}{c}(L-x) + \psi]}{\sin(\frac{\omega}{c}L)} \qquad (A1.3)$$

It also has an unknown phase angle, ϕ, with respect to the mixed response and has an unknown spatial phase shift, ψ. The spatial phase shift is needed to match an ideal standing wave response to the standing wave response component. The scale, B, is the portion of a ideal standing wave response.

A1.3 Equating Responses

These ideal responses associated with an absorptive and a reflective boundary condition are equated, Equation A1.4, to a mixed response associated with a mixed boundary condition that is a combination of absorptive and reflective characteristics.

$$\frac{(-1+K)e^{i\frac{\omega}{c}(x-L)} + (1+K)e^{-i\frac{\omega}{c}(x-L)}}{(-1+K)e^{-i\frac{\omega}{c}L} + (1+K)e^{i\frac{\omega}{c}L}} \tag{A1.4}$$

$$= A\ e^{i(\phi + \frac{\pi}{2} - \frac{\omega}{c}x)} + B\ e^{i\phi}\ \frac{\sin[\frac{\omega}{c}(L-x) + \psi]}{\sin(\frac{\omega}{c}L)}$$

The unknowns to be solved are A, B, ϕ, and ψ.

A is the portion of an ideal propagating wave and B is the portion of an ideal standing wave. The angles, ϕ and ψ, are temporal and spatial phase shifts with respect to the mixed response, which also has a phase angle with respect to the excitation. The scale factor, B, is abstract since it multiplies the ideal standing wave, a term which becomes infinite at a natural frequency. The combined second term of the right-hand side does represent a typical standing wave response.

A1.4 Clearing Fractions

Equation A1.5 is obtained by clearing fractions and gathering similar terms in Equation A1.4. The equality is still preserved. Straight-forward algebraic manipulations are performed on Equation A1.5 to solve for A, B, ϕ, and ψ.

$$[(-1+K)e^{i\frac{\omega}{c}(x-L)} + (1+K)e^{-i\frac{\omega}{c}(x-L)}]\ \sin \frac{\omega}{c}L \tag{A1.5}$$

$$= A\, e^{i(\phi + \frac{\pi}{2} - \frac{\omega}{c}x)} [(-1+K)e^{-i\frac{\omega}{c}L} + (1+K)e^{i\frac{\omega}{c}L}] \sin \frac{\omega}{c}L$$

$$+ B\, [(-1+K)e^{-i\frac{\omega}{c}L} + (1+K)e^{i\frac{\omega}{c}L}] \sin[\frac{\omega}{c}(L-x) + \psi]\, e^{i\phi}$$

The left-hand term, the first term on the right-hand side, and the second term on the right-hand side will be each be expanded separately for convenience.

A1.5 Expanding Left-Hand Side

The left-hand side of Equation A1.5 is expanded first. It is repeated below. First, the complex exponentials are expanded in Equation A1.6.

$$[(-1+K)e^{i\frac{\omega}{c}(x-L)} + (1+K)e^{-i\frac{\omega}{c}(x-L)}] \sin\frac{\omega}{c}L$$

$$= (-1+K) \sin\frac{\omega}{c}L\, [\cos\frac{\omega}{c}(x-L) + i \sin\frac{\omega}{c}(x-L)] \qquad \text{(A1.6)}$$
$$+ (1+K) \sin\frac{\omega}{c}L\, [\cos\frac{\omega}{c}(x-L) - i \sin\frac{\omega}{c}(x-L)]$$

Similar terms are combined, after expanding Equation A1.6, to obtain Equation A1.7.

$$= 2K \sin\frac{\omega}{c}L \cos\frac{\omega}{c}(x-L) - i\, 2\sin\frac{\omega}{c}L \sin\frac{\omega}{c}(x-L) \qquad \text{(A1.7)}$$

It is desirable to separate out the x location dependence. The trigonometric summation terms in Equation A1.7 are expanded and the $\frac{\omega}{c}x$ terms are gathered in Equation A1.8.

$$= (2K \sin\frac{\omega}{c}L \cos\frac{\omega}{c}L) \cos\frac{\omega}{c}x + (2K \sin\frac{\omega}{c}L \sin\frac{\omega}{c}L) \sin\frac{\omega}{c}x \qquad \text{(A1.8)}$$

$$+ i(2\sin\tfrac{\omega}{c}L \sin\tfrac{\omega}{c}L)\cos\tfrac{\omega}{c}x + i(2\sin\tfrac{\omega}{c}L \cos\tfrac{\omega}{c}L)\sin\tfrac{\omega}{c}x$$

Equation A1.8 has four terms each multiplying either $\cos\frac{\omega}{c}x$, $\sin\frac{\omega}{c}x$, $i\cos\frac{\omega}{c}x$, or $i\sin\frac{\omega}{c}x$. The same method will be applied to the two terms on the right-hand side of Equation A1.5.

A1.6 Expanding First Right-Hand Term

The first term on the right-hand side of Equation A1.5 will be expanded now. First, the complex exponentials are expanded and similar terms are gathered in Equation A1.9.

$$A\,e^{i(\phi + \frac{\pi}{2} - \frac{\omega}{c}x)}\left[(-1+K)e^{-i\frac{\omega}{c}L} + (1+K)e^{i\frac{\omega}{c}L}\right]\sin\tfrac{\omega}{c}L$$

$$\begin{aligned} = \quad & - A(-1+K)\sin\tfrac{\omega}{c}L \sin(\phi - \tfrac{\omega}{c}x - \tfrac{\omega}{c}L) \\ & - A\,(1+K)\sin\tfrac{\omega}{c}L \sin(\phi - \tfrac{\omega}{c}x + \tfrac{\omega}{c}L) \\ & + i\,A\,(1+K)\sin\tfrac{\omega}{c}L \cos(\phi - \tfrac{\omega}{c}x - \tfrac{\omega}{c}L) \\ & + i\,A\,(1+K)\sin\tfrac{\omega}{c}L \cos(\phi - \tfrac{\omega}{c}x + \tfrac{\omega}{c}L) \end{aligned} \tag{A1.9}$$

The trigonometric summation of angles in the cosine and sine terms in Equation A1.9 are expanded to separate the $\frac{\omega}{c}x$ dependence. The $\frac{\omega}{c}x$ terms are then collected in Equation A1.10.

$$\begin{aligned} = \quad & \Big[-A(-1+K)\sin\tfrac{\omega}{c}L \sin(\phi - \tfrac{\omega}{c}L) \\ & \qquad - A(1+K)\sin\tfrac{\omega}{c}L \sin(\phi + \tfrac{\omega}{c}L)\Big]\cos\tfrac{\omega}{c}x \\ & + \Big[A(-1+K)\sin\tfrac{\omega}{c}L \cos(\phi - \tfrac{\omega}{c}L) \\ & \qquad + A(1+K)\sin\tfrac{\omega}{c}L \cos(\phi + \tfrac{\omega}{c}L)\Big]\sin\tfrac{\omega}{c}x \\ & + i\Big[A(-1+K)\sin\tfrac{\omega}{c}L \cos(\phi - \tfrac{\omega}{c}L) \\ & \qquad + A(1+K)\sin\tfrac{\omega}{c}L \cos(\phi + \tfrac{\omega}{c}L)\Big]\cos\tfrac{\omega}{c}x \end{aligned} \tag{A1.10}$$

$$+ i\left[A(-1+K)\sin\tfrac{\omega}{c}L \sin(\phi - \tfrac{\omega}{c}L) + A(1+K)\sin\tfrac{\omega}{c}L \sin(\phi + \tfrac{\omega}{c}L)\right] \sin\tfrac{\omega}{c}x$$

Finally, the remaining trigonometric summations in Equation A1.10 are expanded and simplified to obtain Equation A1.11.

$$\begin{aligned} = & \left[-2AK\sin\tfrac{\omega}{c}L \sin\phi \cos\tfrac{\omega}{c}L - 2A\sin^2(\tfrac{\omega}{c}L)\cos\phi\right] \cos\tfrac{\omega}{c}x \\ + & \left[2AK\sin\tfrac{\omega}{c}L \cos\phi \cos\tfrac{\omega}{c}L - 2A\sin^2(\tfrac{\omega}{c}L)\sin\phi\right] \sin\tfrac{\omega}{c}x \\ +i & \left[2AK\sin\tfrac{\omega}{c}L \cos\phi \cos\tfrac{\omega}{c}L - 2A\sin^2(\tfrac{\omega}{c}L)\sin\phi\right] \cos\tfrac{\omega}{c}x \\ +i & \left[2AK\sin\tfrac{\omega}{c}L \sin\phi \cos\tfrac{\omega}{c}L + 2A\sin^2(\tfrac{\omega}{c}L)\cos\phi\right] \sin\tfrac{\omega}{c}x \end{aligned} \qquad \text{(A1.11)}$$

Equation A1.11 also has four terms each multiplying either $\cos\frac{\omega}{c}x$, $\sin\frac{\omega}{c}x$, $i\cos\frac{\omega}{c}x$, or $i\sin\frac{\omega}{c}x$. The only unknowns in Equation A1.11 are A and ϕ.

A1.7 Expanding Second Right-Hand Term

The second right-hand term in Equation A1.5 will be expanded next. The complex exponentials are expanded and multiplication carried out in Equation A1.12.

$$B\left[(-1+K)e^{-i\frac{\omega}{c}L} + (1+K)e^{i\frac{\omega}{c}L}\right] \sin[\tfrac{\omega}{c}(L-x) + \psi]\, e^{i\phi}$$

$$\begin{aligned} = & \; B(-1+K)\sin[\tfrac{\omega}{c}(L-x) + \psi]\left[\cos(\phi - \tfrac{\omega}{c}L) + i\sin(\phi - \tfrac{\omega}{c}L)\right] \\ & + B(1+K)\sin[\tfrac{\omega}{c}(L-x) + \psi]\left[\cos(\phi + \tfrac{\omega}{c}L) + i\sin(\phi + \tfrac{\omega}{c}L)\right] \end{aligned} \qquad \text{(A1.12)}$$

Expanding the trigonometric angle summations involving ϕ in Equation A1.12 and gathering similar terms results in Equation A1.13.

$$= \quad 2BK \sin[\tfrac{\omega}{c}(L-x) + \psi] \left[\cos\phi \cos\tfrac{\omega}{c}L + i2BK \sin\phi \cos\tfrac{\omega}{c}L \right] \qquad (A1.13)$$
$$+ \; 2B \quad \sin[\tfrac{\omega}{c}(L-x) + \psi] \left[-\sin\phi \sin\tfrac{\omega}{c}L + i2BK \cos\phi \sin\tfrac{\omega}{c}L \right]$$

Expanding the trigonometric angle summations involving x in Equation A1.13 and simplifying again results in Equation A1.14.

$$\begin{aligned}
= \; & \Big[2BK \cos\phi \cos\tfrac{\omega}{c}L \, (\sin\tfrac{\omega}{c}L \cos\psi + \cos\tfrac{\omega}{c}L \sin\psi) \qquad (A1.14) \\
& \quad -2B \; \sin\phi \sin\tfrac{\omega}{c}L \, (\sin\tfrac{\omega}{c}L \cos\psi + \cos\tfrac{\omega}{c}L \sin\psi) \Big] \cos\tfrac{\omega}{c}x \\
+ \; & \Big[-2BK \cos\phi \cos\tfrac{\omega}{c}L \, (\cos\tfrac{\omega}{c}L \cos\psi - \sin\tfrac{\omega}{c}L \sin\psi) \\
& \quad +2B \; \sin\phi \sin\tfrac{\omega}{c}L \, (\cos\tfrac{\omega}{c}L \cos\psi + \sin\tfrac{\omega}{c}L \sin\psi) \Big] \sin\tfrac{\omega}{c}x \\
+ i & \Big[2BK \sin\phi \cos\tfrac{\omega}{c}L \, (\sin\tfrac{\omega}{c}L \cos\psi + \cos\tfrac{\omega}{c}L \sin\psi) \\
& \quad +2B \; \cos\phi \sin\tfrac{\omega}{c}L \, (\sin\tfrac{\omega}{c}L \cos\psi + \cos\tfrac{\omega}{c}L \sin\psi) \Big] \cos\tfrac{\omega}{c}x \\
+ i & \Big[-2BK \sin\phi \cos\tfrac{\omega}{c}L \, (\cos\tfrac{\omega}{c}L \cos\psi - \sin\tfrac{\omega}{c}L \sin\psi) \\
& \quad -2B \; \cos\phi \sin\tfrac{\omega}{c}L \, (\cos\tfrac{\omega}{c}L \cos\psi - \sin\tfrac{\omega}{c}L \sin\psi) \Big] \sin\tfrac{\omega}{c}x
\end{aligned}$$

Equation A1.14 has four terms each multiplying either $\cos\frac{\omega}{c}x$, $\sin\frac{\omega}{c}x$, $i\cos\frac{\omega}{c}x$, or $i\sin\frac{\omega}{c}x$.

A1.8 Analytical Method Equations

Equations A1.8, A1.11, and A1.14 are substituted for Equation A1.5 and then the trigonometric terms involving $\frac{\omega}{c}x$ are equated on each side. Equation A1.15 is the $\cos\frac{\omega}{c}x$ term, Equation A1.16 the $\sin\frac{\omega}{c}x$ term, Equation A1.17 the $i\cos\frac{\omega}{c}x$ term, and Equation A1.18 the $i\sin\frac{\omega}{c}x$ term.

$$\begin{aligned}
2K\sin\tfrac{\omega}{c}L \cos\tfrac{\omega}{c}L = \; & -2AK \sin\tfrac{\omega}{c}L \cos\tfrac{\omega}{c}L \sin\phi - 2A\sin^2(\tfrac{\omega}{c}L) \cos\phi \qquad (A1.15) \\
& -2B \; \cos\tfrac{\omega}{c}L \cos\psi \left[\sin\tfrac{\omega}{c}L \sin\phi - K \cos\tfrac{\omega}{c}L \cos\phi \right] \\
& -2B \; \sin\tfrac{\omega}{c}L \sin\psi \left[\sin\tfrac{\omega}{c}L \sin\phi - K \cos\tfrac{\omega}{c}L \cos\phi \right]
\end{aligned}$$

$$2K\sin^2(\tfrac{\omega}{c}L) = 2AK \sin\tfrac{\omega}{c}L \cos\tfrac{\omega}{c}L \cos\phi - 2A\sin^2(\tfrac{\omega}{c}L) \sin\phi$$
$$+2B \cos\tfrac{\omega}{c}L \cos\psi \left[\sin\tfrac{\omega}{c}L \sin\phi - K \cos\tfrac{\omega}{c}L \cos\phi\right]$$
$$-2B \sin\tfrac{\omega}{c}L \sin\psi \left[\sin\tfrac{\omega}{c}L \sin\phi - K \cos\tfrac{\omega}{c}L \cos\phi\right] \quad \text{(A1.16)}$$

$$2 \sin^2(\tfrac{\omega}{c}L) = 2AK \sin\tfrac{\omega}{c}L \cos\tfrac{\omega}{c}L \cos\phi - 2A\sin^2(\tfrac{\omega}{c}L) \sin\phi$$
$$+2B \sin\tfrac{\omega}{c}L \cos\psi \left[K\cos\tfrac{\omega}{c}L \sin\phi + \sin\tfrac{\omega}{c}L \cos\phi\right]$$
$$+2B \cos\tfrac{\omega}{c}L \sin\psi \left[K\cos\tfrac{\omega}{c}L \sin\phi + \sin\tfrac{\omega}{c}L \cos\phi\right] \quad \text{(A1.17)}$$

$$-2 \sin\tfrac{\omega}{c}L \cos\tfrac{\omega}{c}L = 2AK \sin\tfrac{\omega}{c}L \cos\tfrac{\omega}{c}L \sin\phi - 2A\sin^2(\tfrac{\omega}{c}L) \cos\phi$$
$$-2B \cos\tfrac{\omega}{c}L \cos\psi \left[K\cos\tfrac{\omega}{c}L \sin\phi + \sin\tfrac{\omega}{c}L \cos\phi\right]$$
$$+2B \sin\tfrac{\omega}{c}L \sin\psi \left[K\cos\tfrac{\omega}{c}L \sin\phi + \sin\tfrac{\omega}{c}L \cos\phi\right] \quad \text{(A1.18)}$$

A1.9 Solving Analytical Method Equations

The Analytical Method equations, Equations A1.15-A1.18, are solved by direct substitution. First, rearrange Equation A1.16 as shown in Equation A1.19.

$$B(\cos\tfrac{\omega}{c}L \cos\psi - \sin\tfrac{\omega}{c}L \sin\psi) \quad \text{(A1.19)}$$
$$= \frac{K\sin^2(\tfrac{\omega}{c}L) - AK\sin\tfrac{\omega}{c}L \cos\tfrac{\omega}{c}L \cos\phi + A\sin^2(\tfrac{\omega}{c}L) \sin\phi}{\sin\tfrac{\omega}{c}L \sin\phi - K\sin\tfrac{\omega}{c}L \cos\phi}$$

Then, perform a similar rearrangement in Equation A1.18 to obtain the same quantity, in Equation A1.20.

$$B(\cos\tfrac{\omega}{c}L \cos\psi - \sin\tfrac{\omega}{c}L \sin\psi) \quad \text{(A1.20)}$$
$$= \frac{\sin\tfrac{\omega}{c}L \cos\tfrac{\omega}{c}L - AK\sin\tfrac{\omega}{c}L \cos\tfrac{\omega}{c}L \sin\phi - A\sin^2(\tfrac{\omega}{c}L) \cos\phi}{-\sin\tfrac{\omega}{c}L \cos\phi - K\cos\tfrac{\omega}{c}L \sin\phi}$$

Equations A1.19-A1.20 are equated and simplified to obtain the result for ϕ in Equation A1.21.

$$\tan\phi = \frac{-K}{(K^2-1)\sin\frac{\omega}{c}L\,\cos\frac{\omega}{c}L} \qquad \text{(A1.21)}$$

Next, Equation A1.13 is rearranged to obtain Equation A1.22.

$$B(\sin\tfrac{\omega}{c}L\,\cos\psi + \cos\tfrac{\omega}{c}L\,\sin\psi) \qquad \text{(A1.22)}$$

$$= \frac{K\sin\frac{\omega}{c}L\,\cos\frac{\omega}{c}L + AK\sin\frac{\omega}{c}L\,\cos\frac{\omega}{c}L + A\sin^2(\frac{\omega}{c}L)\,\cos\phi}{K\cos\frac{\omega}{c}L\,\cos\phi - \sin\frac{\omega}{c}L\,\sin\phi}$$

Then, Equation A1.18 is similarly rearranged to obtain the same quantity in Equation A1.23.

$$B(\sin\tfrac{\omega}{c}L\,\cos\psi + \cos\tfrac{\omega}{c}L\,\sin\psi) \qquad \text{(A1.23)}$$

$$= \frac{\sin^2(\frac{\omega}{c}L) - AK\sin\frac{\omega}{c}L\,\cos\frac{\omega}{c}L\,\cos\phi + A\sin^2(\frac{\omega}{c}L)\,\sin\phi}{K\cos(\frac{\omega}{c}L)\,\sin\phi - \sin\frac{\omega}{c}L\,\cos\phi}$$

Combining Equations A1.22-A1.23 and simplifying gives a results for A in Equation A1.24.

$$A = -\sin\phi \qquad \text{(A1.24)}$$

Subtracting Equation A1.15 from Equation A1.14 gives the results for B in Equation A1.25.

$$B = \frac{K-1}{(K-1)\frac{1}{\tan\frac{\omega}{c}L}\sin(\psi-\phi) - (1 + K\frac{1}{\tan^2(\frac{\omega}{c}L)})\cos(\psi-\phi)} \qquad \text{(A1.25)}$$

Adding Equation A1.13 and Equation A1.16 gives another result for B in Equation A1.26.

$$B = \frac{K-1}{(K-1)\cos(\psi-\phi) + (\tan\frac{\omega}{c}L + \frac{K}{\tan\frac{\omega}{c}L})\sin(\psi-\phi)} \tag{A1.26}$$

Equating Equations A1.25-A1.26 gives a result for $(\psi-\phi)$ in Equation A1.27.

$$\tan(\psi-\phi) = \frac{-K}{\tan\frac{\omega}{c}L} \tag{A1.27}$$

A1.10 Analytical Method Solutions

The Analytical Method solutions for A, B, ϕ, and ψ that were found above are summarized in Equations A1.28-A1.31.

$$\tan\phi = \frac{-K}{(K^2-1)\sin\frac{\omega}{c}L\ \cos\frac{\omega}{c}L} \tag{A1.28}$$

$$\tan(\psi-\phi) = \frac{-K}{\tan\frac{\omega}{c}L} \tag{A1.29}$$

$$A = -\sin\phi \tag{A1.30}$$

$$B = \frac{K-1}{(K-1)\cos(\psi-\phi) + [\tan\frac{\omega}{c}L + \frac{K}{\tan\frac{\omega}{c}L}]\sin(\psi-\phi)} \tag{A1.31}$$

A, B, ϕ, and ψ are functions of K and, of course, ω, L, and c. Any mixed response can be decomposed into pure propagating and standing wave component responses, if the boundary condition implied by K is specified.

APPENDIX 2

STRIPS METHOD SOLUTIONS

A2.1 Introduction

The STRIPS equations (Equations 4.16-4.19) developed in Chapter 4 will be solved in this appendix. A least squared error technique will be used. Arbitrary values of the propagating and standing wave response components, A, R_1, and R_2, input into the four STRIPS equations will result in non-zero residual errors, E_1, E_2, E_3, and E_4. Exact solutions for the propagating and standing response components will be obtained so that the residual errors are equal to zero.

A2.2 Residual STRIPS Equations

The STRIPS equations, Equations A2.1-A2.4 from Chapter 4 are summarized below. They were developed by assuming that a total acoustic response is composed of the summation of a general model for a propagating and standing wave response component. They are nonlinear in the variables, A, R_1, and R_2.

$$E_1 = A^2 + R_1^2 + 2A\,R_1 \sin(\tfrac{\omega}{c}x_1) - G_{11} \tag{A2.1}$$

$$E_2 = A^2 + R_2^2 + 2A\ R_2 \sin(\tfrac{\omega}{c}x_2) - G_{22} \tag{A2.2}$$

$$E_3 = A^2 \cos(\tfrac{\omega}{c}x_1 - \tfrac{\omega}{c}x_2) + A\ R_1 \sin(\tfrac{\omega}{c}x_2) + A\ R_2 \sin(\tfrac{\omega}{c}x_1) + R_1\ R_2 - \mathrm{Re}(G_{12}) \tag{A2.3}$$

$$E_4 = A^2 \sin(\tfrac{\omega}{c}x_1 - \tfrac{\omega}{c}x_2) + A\ R_1 \cos(\tfrac{\omega}{c}x_2) - A\ R_2 \cos(\tfrac{\omega}{c}x_1) - \mathrm{Im}(G_{12}) \tag{A2.4}$$

Because these equations are non-linear, it is not clear if a solution, or how many solutions, exist. It will be shown that a single, unique solution does exist. Each residual error, E_1, E_2, E_3, and E_4, will be equal to zero when the unknowns, A, R_1, and R_2, have been solved.

A2.3 Squared Residual Error

A least squared error solution technique is applied to Equations A2.1-A2.4 in order to minimize the residual errors. It will be found that the residual errors, E_1, E_2, E_3, and E_4, can be nulled using the STRIPS constraint and conditions found. Each residual error is first squared in Equations A2.5-A2.8. The minimal squared residual error, then, is zero.

$$E_1^2 = -2\ G_{11}\ R_1^2 - 2A^2\ G_{11} + 2A^2\ R_1^2 + 4A\ R_1^3 \sin(\tfrac{\omega}{c}x_1) + 4A^2\ R_1^2 \sin^2(\tfrac{\omega}{c}x_1) + 4A^3\ R_1 \sin(\tfrac{\omega}{c}x_1) - 4A\ G_{11}\ R_1 \sin(\tfrac{\omega}{c}x_1) + A^4 + G_{11}^2 + R_1^4 \tag{A2.5}$$

$$E_2^2 = -2G_{22}\ R_2^2 - 2A^2\ G_{22} + 2A^2\ R_2^2 + 4A\ R_2^3 \sin(\tfrac{\omega}{c}x_2) + 4A^2\ R_2^2 \sin^2(\tfrac{\omega}{c}x_2) + 4A^3\ R_2 \sin(\tfrac{\omega}{c}x_2) - 4A\ G_{22}\ R_2 \sin(\tfrac{\omega}{c}x_2) + A^4 + G_{22}^2 + R_2^4 \tag{A2.6}$$

$$E_3^2 = A^4 \cos^2(\frac{\omega}{c}x_1 - \frac{\omega}{c}x_2) + R_1^2 R_2^2 - 2R_1 R_2 \mathrm{Re}(G_{12}) \tag{A2.7}$$
$$- 2A^2 \mathrm{Re}(G_{12}) \cos(\frac{\omega}{c}x_1 - \frac{\omega}{c}x_2) + A^2 R_1^2 \sin^2(\frac{\omega}{c}x_2)$$
$$+ A^2 R_2^2 \sin^2(\frac{\omega}{c}x_1) - 2A R_1 \mathrm{Re}(G_{12}) \sin(\frac{\omega}{c}x_2)$$
$$+ 2A R_1 R_2^2 \sin(\frac{\omega}{c}x_1) - 2A R_2 \mathrm{Re}(G_{12}) \sin(\frac{\omega}{c}x_1)$$
$$+ 2A R_1^2 R_2 \sin(\frac{\omega}{c}x_2) + 2A^2 R_1 R_2 \cos(\frac{\omega}{c}x_1 - \frac{\omega}{c}x_2)$$
$$+ 2 A^3 R_1 \cos(\frac{\omega}{c}x_1 - \frac{\omega}{c}x_2) \sin(\frac{\omega}{c}x_2)$$
$$+ 2 A^3 R_2 \cos(\frac{\omega}{c}x_1 - \frac{\omega}{c}x_2) \sin(\frac{\omega}{c}x_1)$$
$$+ 2 A^2 R_1 R_2 \sin(\frac{\omega}{c}x_1) \sin(\frac{\omega}{c}x_2) + \mathrm{Re}(G_{12})^2$$

$$E_4^2 = A^4 \sin^2(\frac{\omega}{c}x_1 - \frac{\omega}{c}x_2) - 2A^2 \mathrm{Im}(G_{12}) \sin(\frac{\omega}{c}x_1 - \frac{\omega}{c}x_2) \tag{A2.8}$$
$$+ A^2 R_1^2 \cos^2(\frac{\omega}{c}x_2) + A^2 R_2^2 \cos^2(\frac{\omega}{c}x_1)$$
$$- 2A \mathrm{Im}(G_{12}) R_1 \cos(\frac{\omega}{c}x_2) + 2A \mathrm{Im}(G_{12}) R_2 \cos(\frac{\omega}{c}x_1)$$
$$+ 2 A^3 R_1 \cos(\frac{\omega}{c}x_2) \sin(\frac{\omega}{c}x_1 - \frac{\omega}{c}x_2)$$
$$- 2 A^3 R_2 \cos(\frac{\omega}{c}x_1) \sin(\frac{\omega}{c}x_1 - \frac{\omega}{c}x_2)$$
$$- 2 A^2 R_1 R_2 \cos(\frac{\omega}{c}x_1) \cos(\frac{\omega}{c}x_2) + \mathrm{Im}(G_{12})^2$$

A2.4 Sensitivity Coefficients

Each squared residual error is a function of the unknowns, A, R_1, and R_2. The partial derivatives of each of the four residual equations with respect to the the unknowns, A, R_1, and R_2, are formed in Equations A2.9-A2.20 in order to determine each equation's sensitivity to that variable.

$$\frac{\partial E_1^2}{\partial A} = -4A\, G_{11} + 4A R_1^2 + 4R_1^3 \sin(\frac{\omega}{c}x_1) + 8A R_1^2 \sin^2(\frac{\omega}{c}x_1) \tag{A2.9}$$
$$- 4G_{11} R_1 \sin(\frac{\omega}{c}x_1) + 12 A^2 R_1 \sin(\frac{\omega}{c}x_1) + 4A^3$$

$$\frac{\partial E_1^2}{\partial R_1} = -4G_{11} R_1 + 4A^2 R_1 + 4A^3 \sin(\tfrac{\omega}{c}x_1) - 4A\, G_{11} \sin(\tfrac{\omega}{c}x_1) + 12A\, R_1^2 \sin(\tfrac{\omega}{c}x_1) + 8\, A^2 R_1 \sin^2(\tfrac{\omega}{c}x_1) + 4R_1^3 \tag{A2.10}$$

$$\frac{\partial E_1^2}{\partial R_2} = 0 \tag{A2.11}$$

$$\frac{\partial E_2^2}{\partial A} = -4A\, G_{22} + 4A\, R_2^2 + 4R_2^3 \sin(\tfrac{\omega}{c}x_2) + 8A\, R_2^2 \sin^2(\tfrac{\omega}{c}x_2) - 4G_{22} R_2 \sin(\tfrac{\omega}{c}x_2) + 12A^2 R_2 \sin(\tfrac{\omega}{c}x_2) + 4A^3 \tag{A2.12}$$

$$\frac{\partial E_2^2}{\partial R_1} = 0 \tag{A2.13}$$

$$\frac{\partial E_2^2}{\partial R_2} = -4G_{22} R_2 + 4A^2 R_2 + 4A^3 \sin(\tfrac{\omega}{c}x_2) - 4A\, G_{22} \sin(\tfrac{\omega}{c}x_2) + 12A\, R_2^2 \sin(\tfrac{\omega}{c}x_2) + 8A^2 R_2 \sin^2(\tfrac{\omega}{c}x_2) + 4R_2^3 \tag{A2.14}$$

$$\begin{aligned}\frac{\partial E_3^2}{\partial A} = {} & 4\, A^3 \cos^2(\tfrac{\omega}{c}x_1 - \tfrac{\omega}{c}x_2) - 4A\, \mathrm{Re}(G_{12}) \cos(\tfrac{\omega}{c}x_1 - \tfrac{\omega}{c}x_2) \\ & + 2A\, R_1^2 \sin^2(\tfrac{\omega}{c}x_2) + 2A\, R_2^2 \sin^2(\tfrac{\omega}{c}x_1) \\ & - 2R_1 \mathrm{Re}(G_{12}) \sin(\tfrac{\omega}{c}x_2) + 2R_1 R_2^2 \sin(\tfrac{\omega}{c}x_1) \\ & - 2R_2 \mathrm{Re}(G_{12}) \sin(\tfrac{\omega}{c}x_1) + 2\, R_1^2 R_2 \sin(\tfrac{\omega}{c}x_2) \\ & + 4A\, R_1 R_2 \cos(\tfrac{\omega}{c}x_1 - \tfrac{\omega}{c}x_2) \\ & + 6\, A^2 R_1 \cos(\tfrac{\omega}{c}x_1 - \tfrac{\omega}{c}x_2) \sin(\tfrac{\omega}{c}x_2) \\ & + 6\, A^2 R_2 \cos(\tfrac{\omega}{c}x_1 - \tfrac{\omega}{c}x_2) \sin(\tfrac{\omega}{c}x_1) \\ & + 4A\, R_1 R_2 \sin(\tfrac{\omega}{c}x_1) \sin(\tfrac{\omega}{c}x_2)\end{aligned} \tag{A2.15}$$

$$\begin{aligned}\frac{\partial E_3^2}{\partial R_1} = {} & 2R_1 R_2^2 - 2R_2 \mathrm{Re}(G_{12}) - 2A\, \mathrm{Re}(G_{12}) \sin(\tfrac{\omega}{c}x_2) \\ & + 2A\, R_2^2 \sin(\tfrac{\omega}{c}x_1) + 2A^2 R_1 \sin^2(\tfrac{\omega}{c}x_2) \\ & + 2A^2 R_2 \cos(\tfrac{\omega}{c}x_1 - \tfrac{\omega}{c}x_2) \\ & + 2A^3 \cos(\tfrac{\omega}{c}x_1 - \tfrac{\omega}{c}x_2) \sin(\tfrac{\omega}{c}x_2)\end{aligned} \tag{A2.16}$$

$$+ 4A R_1 R_2 \sin(\tfrac{\omega}{c}x_2) + 2A^2 R_2 \sin(\tfrac{\omega}{c}x_1) \sin(\tfrac{\omega}{c}x_2)$$

$$\frac{\partial E_3^2}{\partial R_2} = -2R_1 \mathrm{Re}(G_{12}) + 2R_1^2 R_2 - 2A \mathrm{Re}(G_{12}) \sin(\tfrac{\omega}{c}x_1) \tag{A2.17}$$
$$+ 2A R_1^2 \sin(\tfrac{\omega}{c}x_2) + 2A^2 R_1 \cos(\tfrac{\omega}{c}x_1 - \tfrac{\omega}{c}x_2)$$
$$+ 2A^2 R_2 \sin^2(\tfrac{\omega}{c}x_1) + 2A^3 \cos(\tfrac{\omega}{c}x_1 - \tfrac{\omega}{c}x_2) \sin(\tfrac{\omega}{c}x_1)$$
$$+ 4A R_1 R_2 \sin(\tfrac{\omega}{c}x_1) + 2A^2 R_1 \sin(\tfrac{\omega}{c}x_1) \sin(\tfrac{\omega}{c}x_2)$$

$$\frac{\partial E_4^2}{\partial A} = 4A^3 \sin^2(\tfrac{\omega}{c}x_1 - \tfrac{\omega}{c}x_2) - 4A \mathrm{Im}(G_{12}) \sin(\tfrac{\omega}{c}x_1 - \tfrac{\omega}{c}x_2) \tag{A2.18}$$
$$+ 2A R_1^2 \cos^2(\tfrac{\omega}{c}x_2) + 2A R_2^2 \cos^2(\tfrac{\omega}{c}x_1)$$
$$- 2\mathrm{Im}(G_{12}) R_1 \cos(\tfrac{\omega}{c}x_2) + 2\mathrm{Im}(G_{12}) R_2 \cos(\tfrac{\omega}{c}x_1)$$
$$+ 6A^2 R_1 \cos(\tfrac{\omega}{c}x_2) \sin(\tfrac{\omega}{c}x_1 - \tfrac{\omega}{c}x_2)$$
$$- 6A^2 R_2 \cos(\tfrac{\omega}{c}x_1) \sin(\tfrac{\omega}{c}x_1 - \tfrac{\omega}{c}x_2)$$
$$- 4A R_1 R_2 \cos(\tfrac{\omega}{c}x_1) \cos(\tfrac{\omega}{c}x_2)$$

$$\frac{\partial E_4^2}{\partial R_1} = -2A \mathrm{Im}(G_{12}) \cos(\tfrac{\omega}{c}x_2) + 2 A^2 R_1 \cos^2(\tfrac{\omega}{c}x_2) \tag{A2.19}$$
$$+ 2 A^3 \cos(\tfrac{\omega}{c}x_2) \sin(\tfrac{\omega}{c}x_1 - \tfrac{\omega}{c}x_2)$$
$$- 2 A^2 R_2 \cos(\tfrac{\omega}{c}x_1) \cos(\tfrac{\omega}{c}x_2)$$

$$\frac{\partial E_4^2}{\partial R_2} = 2A \mathrm{Im}(G_{12}) \cos(\tfrac{\omega}{c}x_1) + 2 A^2 R_2 \cos^2(\tfrac{\omega}{c}x_1) \tag{A2.20}$$
$$- 2 A^3 \cos(\tfrac{\omega}{c}x_1) \sin(\tfrac{\omega}{c}x_1 - \tfrac{\omega}{c}x_2)$$
$$- 2 A^2 R_1 \cos(\tfrac{\omega}{c}x_1) \cos(\tfrac{\omega}{c}x_2)$$

A2.5 Extremizing Squared Residual Error

The sensitivity equations, Equations A2.9-A2.20, are each factored and summarized below in Equations A2.21-A2.32. The squared residual errors are insensitive to the unknowns when all of the sensitivity coefficients are equal to zero. Some of the squared errors are already insensitive to the unknowns. This is also the same as extremizing the squared residual errors by the unknowns, A, R_1, and R_2, at values where the partial derivatives are equal to zero.

$$\frac{\partial E_1^2}{\partial A} = 0 = 4\left[A + R_1 \sin(\tfrac{\omega}{c}x_1)\right] \cdot \left[R_1^2 + 2A\, R_1 \sin(\tfrac{\omega}{c}x_1) + A^2 - G_{11}\right] \tag{A2.21}$$

$$\frac{\partial E_1^2}{\partial R_1} = 0 = 4\left[R_1 + A \sin(\tfrac{\omega}{c}x_1)\right] \cdot \left[R_1^2 + 2A\, R_1 \sin(\tfrac{\omega}{c}x_1) + A^2 - G_{11}\right] \tag{A2.22}$$

$$\frac{\partial E_1^2}{\partial R_2} = 0 \tag{A2.23}$$

$$\frac{\partial E_2^2}{\partial A} = 0 = 4\left[A + R_2 \sin(\tfrac{\omega}{c}x_2)\right] \cdot \left[R_2^2 + 2A\, R_2 \sin(\tfrac{\omega}{c}x_2) + A^2 - G_{22}\right] \tag{A2.24}$$

$$\frac{\partial E_2^2}{\partial R_1} = 0 \tag{A2.25}$$

$$\frac{\partial E_2^2}{\partial R_2} = 0 = 4\left[R_2 + A \sin(\tfrac{\omega}{c}x_2)\right] \cdot \left[R_2^2 + 2A\, R_2 \sin(\tfrac{\omega}{c}x_2) + A^2 - G_{22}\right] \tag{A2.26}$$

$$\begin{aligned}\frac{\partial E_3^2}{\partial A} = 0 = 2&\left[2A \cos(\tfrac{\omega}{c}x_1 - \tfrac{\omega}{c}x_2) + R_1 \sin(\tfrac{\omega}{c}x_2) + R_2 \sin(\tfrac{\omega}{c}x_1)\right] \\ &\cdot \left[-\mathrm{Re}(G_{12}) + R_1\, R_2 + A^2 \cos(\tfrac{\omega}{c}x_1 - \tfrac{\omega}{c}x_2) + A\, R_1 \sin(\tfrac{\omega}{c}x_2) \right. \\ &\qquad \left. + A\, R_2 \sin(\tfrac{\omega}{c}x_1)\right]\end{aligned} \tag{A2.27}$$

$$\frac{\partial E_3^2}{\partial R_1} = 0 = 2\left[R_2 + A\sin(\tfrac{\omega}{c}x_2)\right] \tag{A2.28}$$
$$\cdot \left[-\mathrm{Re}G_{12} + R_1 R_2 + A^2 \cos(\tfrac{\omega}{c}x_1 - \tfrac{\omega}{c}x_2) + A R_1 \sin(\tfrac{\omega}{c}x_2) + A R_2 \sin(\tfrac{\omega}{c}x_1)\right]$$

$$\frac{\partial E_3^2}{\partial R_2} = 0 = 2\left[R_2 + A\sin(\tfrac{\omega}{c}x_1)\right] \tag{A2.29}$$
$$\cdot \left[-\mathrm{Re}(G_{12}) + R_1 R_2 + A^2 \cos(\tfrac{\omega}{c}x_1 - \tfrac{\omega}{c}x_2) + A R_1 \sin(\tfrac{\omega}{c}x_2) + A R_2 \sin(\tfrac{\omega}{c}x_1)\right]$$

$$\frac{\partial E_4^2}{\partial A} = 0 = 2\left[2A\sin(\tfrac{\omega}{c}x_1 - \tfrac{\omega}{c}x_2) + R_1\cos(\tfrac{\omega}{c}x_2) - R_2\cos(\tfrac{\omega}{c}x_1)\right] \tag{A2.30}$$
$$\cdot \left[-\mathrm{Im}(G_{12}) + A^2 \sin(\tfrac{\omega}{c}x_1 - \tfrac{\omega}{c}x_2) + A R_1 \cos(\tfrac{\omega}{c}x_2) - A R_2 \cos(\tfrac{\omega}{c}x_1)\right]$$

$$\frac{\partial E_4^2}{\partial R_1} = 0 = 2A\cos(\tfrac{\omega}{c}x_2) \tag{A2.31}$$
$$\cdot \left[-\mathrm{Im}(G_{12}) + A^2 \sin(\tfrac{\omega}{c}x_1 - \tfrac{\omega}{c}x_2) + A R_1 \cos(\tfrac{\omega}{c}x_2) - A R_2 \cos(\tfrac{\omega}{c}x_1)\right]$$

$$\frac{\partial E_4^2}{\partial R_2} = 0 = -2A\cos(\tfrac{\omega}{c}x_1) \tag{A2.32}$$
$$\cdot \left[-\mathrm{Im}(G_{12}) + A^2 \sin(\tfrac{\omega}{c}x_1 - \tfrac{\omega}{c}x_2) + A R_1 \cos(\tfrac{\omega}{c}x_2) - A R_2 \cos(\tfrac{\omega}{c}x_1)\right]$$

A2.6 Minimized Squared Residual Error

Four common factors (Equations A2.33-A2.36) are found in the twelve equations above. When they are all equal to zero, then all twelve of the partial derivatives are also equal to zero. The squared residual error is then extremized.

$$0 = R_1^2 + 2A\,R_1 \sin(\tfrac{\omega}{c}x_1) + A^2 - G_{11} \qquad \text{(A2.33)}$$

$$0 = R_2^2 + 2A\,R_2 \sin(\tfrac{\omega}{c}x_2) + A^2 - G_{22} \qquad \text{(A2.34)}$$

$$0 = -\mathrm{Re}(G_{12}) + R_1\,R_2 + A^2 \cos(\tfrac{\omega}{c}x_1 - \tfrac{\omega}{c}x_2) + A\,R_1 \sin(\tfrac{\omega}{c}x_2) + A\,R_2 \sin(\tfrac{\omega}{c}x_1) \qquad \text{(A2.35)}$$

$$0 = -\mathrm{Im}(G_{12}) + A^2 \sin(\tfrac{\omega}{c}x_1 - \tfrac{\omega}{c}x_2) + A\,R_1 \cos(\tfrac{\omega}{c}x_2) - A\,R_2 \cos(\tfrac{\omega}{c}x_1) \qquad \text{(A2.36)}$$

First, solve Equation A2.33 for R_1. The result is in terms of A.

$$R_1 = -A \sin(\tfrac{\omega}{c}x_1) \pm \left[A^2 \sin^2(\tfrac{\omega}{c}x_1) - (A^2 - G_{11})\right]^{0.5}$$

$$= -A \sin(\tfrac{\omega}{c}x_1) \pm \left[-A^2 \cos^2(\tfrac{\omega}{c}x_1) + G_{11}\right]^{0.5} \qquad \text{(A2.37)}$$

Then, solve Equation A2.34 for R_2.

$$R_2 = -A \sin(\tfrac{\omega}{c}x_2) \pm \left[A^2 \sin^2(\tfrac{\omega}{c}x_2) - (A^2 - G_{22})\right]^{0.5}$$

$$= -A \sin(\tfrac{\omega}{c}x_2) \pm \left[-A^2 \cos^2(\tfrac{\omega}{c}x_2) + G_{22}\right]^{.5} \qquad \text{(A2.38)}$$

Putting Equations A2.37-A2.38 into Equation A2.35 results in

$$\left[-A^2 \cos^2(\tfrac{\omega}{c}x_1) + G_{11}\right]^{0.5}\left[-A^2 \cos^2(\tfrac{\omega}{c}x_2) + G_{22}\right]^{0.5} = \left[\mathrm{Re}(G_{12}) - A^2 \cos(\tfrac{\omega}{c}x_1) \cos(\tfrac{\omega}{c}x_2)\right] \qquad \text{(A2.39)}$$

Putting Equations A2.37-A2.38 also into Equation A2.36 results in

$$\mathrm{Im}(G_{12}) = A \cos(\tfrac{\omega}{c}x_1) \left[-A^2 \cos^2(\tfrac{\omega}{c}x_2) + G_{22}\right]^{0.5} - A \cos(\tfrac{\omega}{c}x_2) \left[-A^2 \cos^2(\tfrac{\omega}{c}x_1) + G_{11}\right]^{0.5} \qquad \text{(A2.40)}$$

Squaring both sides of Equation A2.40 gives

$$\begin{aligned}\mathrm{Im}(G_{12})^2 = {} & A^2\cos^2(\tfrac{\omega}{c}x_1)\left[-A^2\cos^2(\tfrac{\omega}{c}x_2) + G_{22}\right] \\ & + A^2\cos^2(\tfrac{\omega}{c}x_2)\left[-A^2\cos^2(\tfrac{\omega}{c}x_1) + G_{11}\right] \\ & -2A^2\cos(\tfrac{\omega}{c}x_1)\cos(\tfrac{\omega}{c}x_2)\left[-A^2\cos^2(\tfrac{\omega}{c}x_1) + G_{11}\right]^{0.5}\left[-A^2\cos^2(\tfrac{\omega}{c}x_2) + G_{22}\right]^{0.5}\end{aligned} \tag{A2.41}$$

Substituting Equation A2.39 into Equation A2.41

$$\begin{aligned}\mathrm{Im}(G_{12})^2 = {} & A^2\cos^2(\tfrac{\omega}{c}x_1)\left[-A^2\cos^2(\tfrac{\omega}{c}x_2) + G_{22}\right] \\ & + A^2\cos^2(\tfrac{\omega}{c}x_2)\left[-A^2\cos^2(\tfrac{\omega}{c}x_1) + G_{11}\right] \\ & - 2A^2\cos(\tfrac{\omega}{c}x_1)\cos(\tfrac{\omega}{c}x_2)\left[\mathrm{Re}(G_{12}) - A^2\cos(\tfrac{\omega}{c}x_1)\cos(\tfrac{\omega}{c}x_2)\right]\end{aligned} \tag{A2.42}$$

Expanding and simplifying Equation A2.42

$$\begin{aligned}\mathrm{Im}(G_{12})^2 = A^2 \Big[& G_{11}\cos^2(\tfrac{\omega}{c}x_2) + G_{22}\cos^2(\tfrac{\omega}{c}x_1) \\ & - 2\mathrm{Re}(G_{12})\cos(\tfrac{\omega}{c}x_1)\cos(\tfrac{\omega}{c}x_2)\Big]\end{aligned} \tag{A2.43}$$

Solving this for A gives

$$A^2 = \frac{\mathrm{Im}(G_{12})^2}{G_{11}\cos^2(\tfrac{\omega}{c}x_2) + G_{22}\cos^2(\tfrac{\omega}{c}x_1) - 2\mathrm{Re}(G_{12})\cos\tfrac{\omega}{c}x_1\cos\tfrac{\omega}{c}x_2} \tag{A2.44}$$

This equation along with R_1 and R_2 already developed are the STRIPS method solutions.

$$R_1 = \quad = -A\sin(\tfrac{\omega}{c}x_1) \pm \left[-A^2\cos^2(\tfrac{\omega}{c}x_1) + G_{11}\right]^{0.5} \tag{A2.45}$$

$$R_2 = \quad = -A \sin(\tfrac{\omega}{c}x_2) \pm \left[A^2 \cos^2(\tfrac{\omega}{c}x_2) + G_{22}\right]^{0.5} \tag{A2.46}$$

A2.7 STRIPS Constraint and Conditions

Equations A2.44-A2.46 extremize the squared residual error in any of the STRIPS equations. It is desirable to determine the combination that results in a minimum, and possibly a zero, residual error. Substitute Equations A2.44-A2.46 back into the STRIPS equations, Equations A2.1-A2.4. The first two STRIPS equations (Equations A2.1-A2.2) are satisfied exactly, as shown in Equations A2.47-A2.48.

$$E_1 = 0 \tag{A2.47}$$

$$E_2 = 0 \tag{A2.48}$$

The third STRIPS equation (Equation A2.3) is simplified into the form shown in Equation A2.49.

$$E_3 = \frac{\left\{ \begin{array}{l} \left[G_{11}^2 \cos^2(\tfrac{\omega}{c}x_2) - \mathrm{Im}(G_{12})^2 \cos^2(\tfrac{\omega}{c}x_1) + G_{11}G_{22} \cos^2(\tfrac{\omega}{c}x_1) \right. \\ \qquad \left. -2G_{11}\,\mathrm{Re}(G_{12}) \cos(\tfrac{\omega}{c}x_1) \cos(\tfrac{\omega}{c}x_2)\right]^{0.5} \\ \cdot \left[G_{22}^2 \cos^2(\tfrac{\omega}{c}x_1) - \mathrm{Im}(G_{12})^2 \cos^2(\tfrac{\omega}{c}x_2) + G_{11}G_{22} \cos^2(\tfrac{\omega}{c}x_2) \right. \\ \qquad \left. -2G_{22}\,\mathrm{Re}(G_{12}) \cos(\tfrac{\omega}{c}x_1) \cos(\tfrac{\omega}{c}x_2)\right]^{0.5} \\ \mp G_{11}\,\mathrm{Re}(G_{12}) \cos^2(\tfrac{\omega}{c}x_2) \mp G_{22}\,\mathrm{Re}(G_{12}) \cos^2(\tfrac{\omega}{c}x_1) \\ \pm \mathrm{Im}(G_{12})^2 \cos(\tfrac{\omega}{c}x_1) \cos(\tfrac{\omega}{c}x_2) \pm 2\mathrm{Re}(G_{12})^2 \cos(\tfrac{\omega}{c}x_1) \cos(\tfrac{\omega}{c}x_2) \end{array} \right\}}{G_{11} \cos^2(\tfrac{\omega}{c}x_2) + G_{22} \cos^2(\tfrac{\omega}{c}x_1) - 2\mathrm{Re}(G_{12}) \cos(\tfrac{\omega}{c}x_1) \cos(\tfrac{\omega}{c}x_2)} \tag{A2.49}$$

The $\mp$ and $\pm$ signs are dependent on which sign is chosen in Equation A2.45, R_1, and Equation A2.46, R_2. The top sign results if the the same sign was chosen in both R_1 and R_2. The bottom sign results if the opposite sign was chosen in R_1 and R_2. The STRIPS constraint in Equation A2.50 is found when the numerator of E_3, Equation A2.49, is equated to zero.

$$G_{11}\ G_{22} = \mathrm{Im}(G_{12})^2 + \mathrm{Re}(G_{12})^2 \tag{A2.50}$$

Substituting the STRIPS constraint into E_3 results in Equation A2.51. The signs of the two terms in the first product determine which of the two plus-minus signs is appropriate for the later terms.

$$\begin{aligned} 0 = &\left[\mathrm{Re}(G_{12})\cos(\tfrac{\omega}{c}x_1) - G_{11}\cos(\tfrac{\omega}{c}x_2)\right] \\ &\qquad \cdot \left[\mathrm{Re}(G_{12})\cos(\tfrac{\omega}{c}x_1) - G_{22}\cos(\tfrac{\omega}{c}x_1)\right] \\ &\mp G_{11}\,\mathrm{Re}(G_{12})\cos^2(\tfrac{\omega}{c}x_2) \mp G_{22}\,\mathrm{Re}(G_{12})\cos^2(\tfrac{\omega}{c}x_1) \\ &\pm \mathrm{Im}(G_{12})^2\cos(\tfrac{\omega}{c}x_1)\cos(\tfrac{\omega}{c}x_2) \pm 2\mathrm{Re}(G_{12})^2\cos(\tfrac{\omega}{c}x_1)\cos(\tfrac{\omega}{c}x_2) \end{aligned} \tag{A2.51}$$

If the first two terms result in a negative product, then the top signs must be chosen if the numerator is to be zero. It the first two terms results in a positive product, then the bottom signs must be chosen. These STRIPS conditions will be met depending on the relative magnitude of the differences contained in the first two terms, as shown in Equations A2.52-A2.53.

<u>CONDITION</u>	<u>SIGN SELECTION</u>		
	Equation A2.45	Equation A2.46	
$G_{11}\ \mathrm{Cos}(\frac{\omega}{c}x_2) \lessgtr \mathrm{Re}(G_{12})\ \mathrm{Cos}(\frac{\omega}{c}x_1)$	$\pm$	$\pm$	(A2.52)
$G_{22}\ \mathrm{Cos}(\frac{\omega}{c}x_1) \gtrless \mathrm{Re}(G_{12})\ \mathrm{Cos}(\frac{\omega}{c}x_2)$			
$G_{11}\ \mathrm{Cos}(\frac{\omega}{c}x_2) \gtrless \mathrm{Re}(G_{12})\ \mathrm{Cos}(\frac{\omega}{c}x_1)$	$\mp$	$\pm$	(A2.53)

$$G_{22}\ \cos(\tfrac{\omega}{c}x_1) \ \gtrless\ \mathrm{Re}(G_{12})\ \cos(\tfrac{\omega}{c}x_2)$$

Substituting the STRIPS solutions, Equations A2.44-A2.46, into E_4 in Equation A2.4 and simplifying results in Equation A2.54. In the two ± selections in Equation A2.54, a plus-minus combination is a result of selecting a plus in R_1 and a plus in R_2. A plus-plus combination is a result of selecting a minus in R_1 and a plus in R_2. A minus-plus combination is a result of selecting a minus in R_1 and a minus in R_2. A minus-minus combination is a result of selecting a plus in R_1 and a minus in R_2.

$$E_4 = \frac{\begin{aligned}-\mathrm{Im}(G_{12})\Big\{ & G_{11}\cos^2(\tfrac{\omega}{c}x_2) + G_{22}\cos^2(\tfrac{\omega}{c}x_1) - 2\mathrm{Re}(G_{12})\cos(\tfrac{\omega}{c}x_1)\cos(\tfrac{\omega}{c}x_2) \\ & \pm \cos(\tfrac{\omega}{c}x_1)\Big[G_{22}^2\cos^2(\tfrac{\omega}{c}x_1) - \mathrm{Im}(G_{12})^2\cos^2(\tfrac{\omega}{c}x_2) \\ & \quad + G_{11}G_{22}\cos^2(\tfrac{\omega}{c}x_2) - 2G_{22}\ \mathrm{Re}(G_{12})\cos(\tfrac{\omega}{c}x_1)\cos(\tfrac{\omega}{c}x_2)\Big]^{0.5} \\ & \pm \cos(\tfrac{\omega}{c}x_2)\Big[G_{11}^2\cos^2(\tfrac{\omega}{c}x_2) - \mathrm{Im}(G_{12})^2\cos^2(\tfrac{\omega}{c}x_1) \\ & \quad + G_{11}G_{22}\cos^2(\tfrac{\omega}{c}x_1) - 2G_{22}\mathrm{Re}(G_{12})\cos(\tfrac{\omega}{c}x_1)\cos(\tfrac{\omega}{c}x_2)\Big]^{0.5}\Big\}\end{aligned}}{G_{11}\ \cos^2(\tfrac{\omega}{c}x_2) + G_{22}\ \cos^2(\tfrac{\omega}{c}x_1) - 2\mathrm{Re}(G_{12})\ \cos(\tfrac{\omega}{c}x_1)\ \cos(\tfrac{\omega}{c}x_2)} \tag{A2.54}$$

Putting the STRIPS constraint of Equation A2.50 into E_4 in Equation A2.54 and equating the numerator to zero results in Equation A2.55.

$$\begin{aligned} 0 = & \Big[G_{11}\cos^2(\tfrac{\omega}{c}x_2) + G_{22}\cos^2(\tfrac{\omega}{c}x_1) - 2\mathrm{Re}(G_{12})\cos(\tfrac{\omega}{c}x_1)\cos(\tfrac{\omega}{c}x_2)\Big] \\ & \pm \cos(\tfrac{\omega}{c}x_1)\ \Big[\mathrm{Re}(G_{12})\cos(\tfrac{\omega}{c}x_2) - G_{22}\cos(\tfrac{\omega}{c}x_1)\Big] \\ & \pm \cos(\tfrac{\omega}{c}x_2)\ \Big[\mathrm{Re}(G_{12})\cos(\tfrac{\omega}{c}x_1) - G_{11}\cos(\tfrac{\omega}{c}x_2)\Big] \end{aligned} \tag{A2.55}$$

The plus-minus signs chosen depend on the relative magnitude of the differences contained in the last two terms. They are summarized in Equations A2.56-A2.59.

CONDITION	SIGN SELECTION		
	Equation A2.45	Equation A2.46	
$G_{11}\ \mathrm{Cos}(\frac{\omega}{c}x_2) < \mathrm{Re}(G_{12})\ \mathrm{Cos}(\frac{\omega}{c}x_1)$ $G_{22}\ \mathrm{Cos}(\frac{\omega}{c}x_1) > \mathrm{Re}(G_{12})\ \mathrm{Cos}(\frac{\omega}{c}x_2)$	+	+	(A2.56)
$G_{11}\ \mathrm{Cos}(\frac{\omega}{c}x_2) < \mathrm{Re}(G_{12})\ \mathrm{Cos}(\frac{\omega}{c}x_1)$ $G_{22}\ \mathrm{Cos}(\frac{\omega}{c}x_1) < \mathrm{Re}(G_{12})\ \mathrm{Cos}(\frac{\omega}{c}x_2)$	+	-	(A2.57)
$G_{11}\ \mathrm{Cos}(\frac{\omega}{c}x_2) > \mathrm{Re}(G_{12})\ \mathrm{Cos}(\frac{\omega}{c}x_1)$ $G_{22}\ \mathrm{Cos}(\frac{\omega}{c}x_1) > \mathrm{Re}(G_{12})\ \mathrm{Cos}(\frac{\omega}{c}x_2)$	-	+	(A2.58)
$G_{11}\ \mathrm{Cos}(\frac{\omega}{c}x_2) > \mathrm{Re}(G_{12})\ \mathrm{Cos}(\frac{\omega}{c}x_1)$ $G_{22}\ \mathrm{Cos}(\frac{\omega}{c}x_1) < \mathrm{Re}(G_{12})\ \mathrm{Cos}(\frac{\omega}{c}x_2)$	-	-	(A2.59)

These four STRIPS conditions in conjunction with the STRIPS solutions, Equation A2.44-A2.46 insure that the residual errors are equal to zero. The STRIPS solutions are exact solutions.

LIST OF REFERENCES

LIST OF REFERENCES

1. M.C. Rodamaker, "Measurement versus Simulation", Sound and Vibration, November, p. 5, (1984).

2. A.H. Suter, "Legal Status of the Hearing Conservation Amendment and Its effects on the CQ", Sound and Vibration, December, 4-5, (1985).

3. G. Porges, Applied Acoustics, John Wiley, New York, (1977).

4. S. Temkin, Elements of Acoustics, John Wiley, New York, (1981).

5. V.S. Mankovsky, Acoustics of Studios and Auditoria, Hastings House, New York, (1971).

6. B.G. van Zyl, F. Anderson, and P.J. Erasmus, "Sound Intensity in Diffuse Sound Fields", J. Acoust. Soc. Am. 78(2), 587-589, (1985).

7. J. Nicolas, and G. Lemire, "Precision of Active Sound Intensity Measurements in a Progressive and a Nonprogressive Field", J. Acoust. Soc. Am. 78(2), 414-422, (1985).

8. S. Takagi, T. Nakamura, and Y. Irie, "A Measuring Method of Acoustic Intensity of Forward and Backward Propagating Waves", Am. Soc. of Mech. Engineers, 85-DET-158, ASME Design, Engineering Division Conference, Cincinnati, Ohio, September, (1985).

9. J. Tichy, "Acoustic Intensity Measurements - A Review", AIAA/NASA 9th Aeroacoustics Conference, Williamsburg, Virginia, October 15-17, (1984).

10. F.J. Fahy, "Measurement of Acoustic Intensity Using the Cross-Spectral Density of Two-Microphone Signals", J. Acoust. Soc. Amer. 62(4), 1057-1059 (L), (1977).

11. J.Y. Chung, "Cross-spectral Method of Measuring Acoustic Intensity Without Error caused by Instrument Phase Mismatch", J. Acoust. Soc. Amer. 64(6), 1613-1616, (1978).

12. S. Gade, "Sound Intensity (Theory)", Technical Review, Bruel & Kjaer Instruments Inc., No. 3, (1982).

13. E. Zauderer, "Partial Differential Equations of Applied Mathematics", John Wiley and Sons, New York, (1983).

14. M.K. Au-Yang, "Pump-Induced Acoustic Pressure Distribution in an Annular Cavity Bounded by Rigid Walls", J. Sound and Vibration 62(4), 577-591, (1979).

15. R. Singh, "Acoustic Impedance Measurement Methods", Shock and Vibration Digest 14(2), 3-9, (1982).

16. American Society for Testing and Materials, "Impedance and Absorption of Acoustical Materials by the Impedance Tube Method", ASTM C384-85, 1985 Annual Book of ASTM Standards, 4.06(4), (1985).

17. M.D. Dahl, and E.J. Rice, "Measured Acoustic Properties of Variable and Low Sensity Bulk Absorbers", Am. Soc. of Mech. Engineers, 85-WA/NCA-6, ASME Winter Annual Meeting, Miami Beach, Florida, (1985).

18. A.F. Seybert, and D.F. Ross, "Experimental Determination of Acoustic Properties Using a Two-Microphone Random-Excitation Technique", J. of Acoust. Soc. Am. 61(5), 1362-1370, (1977).

19. J. Dunlop, "An Open Tube Technique for the Measurement of Acoustic Parameters of Porous Absorbing Materials", J. Acoust. Soc. Am. 77(6), 2173-2178, (1985).

20. J.F. Allard, and S. Sieben, "Measurement of Acoustic Impedance in a Free Field with Two Microphones and a Spectrum Analyzer", J. Acoust. Soc. Am. 77(4), 1617-1618, (1985).

21. S.H. Sung, "Automotive Applications of Three-Dimensional Acoustic Finite Element Methods", Society of Automotive Engineers, SAE Paper No. 810397, (1981).

22. D.J. Nefske, J.A. Wolf, Jr., and L.J. Howell, "Structural Acoustic Finite Element Analysis of the Automobile Passenger Compartment: A Review of Current Practice", Journal of Sound and Vibration 80(2), 247-266, (1982).

23. A.L. Klosterman, W.A. McCleland, and J.E. Sherlock, "Dynamic Simulation of Complex Systems Utilizing Experimental and Analytical Techniques", ASME 75-WA/Aero-9, (1975).

24. M. Richardson, and J. Kniskern, "Identifying Modes of Large Structures from Multiple Input and Response Measurements", SAE 760875, (1976).

25. J.J. Nieter, and R. Singh, "Acoustic Modal Analysis Experiment", J. Acous. Soc. Am. 72(2), 319-326, (1982).

26. C. Kung, and R. Singh, "Experimental Modal Analysis Technique for Three-Dimensional Acoustic Cavities", J. Acoust. Soc. Am. 77(2), 731-738, (1985).

27. P.M. Morse, and K.U. Ingard, Theoretical Acoustics, McGraw-Hill Book Company, New York, (1968).

28. L.L. Beranek, Noise and Vibration Control, McGraw-Hill Book Company, New York, (1971).

29. L.E. Kinsler, and A.R. Frey, Fundamentals of Acoustics, John Wiley and Sons, New York, (1962).

30. A.D. Pierce, Acoustics, An Introduction to Its Physical Princples and Applications, McGraw-Hill Book Company, New York, (1981).

31. J.L. Hunter, Acoustics, Prentice-Hall Inc., Englewood Cliffs, N.J., (1957).

32. L.L. Beranek, Noise Reduction, McGraw-Hill Book Company, New York, (1960).

33. L.L. Beranek, Acoustics, McGraw-Hill Book Company, New York, (1954).

34. R.V. Churchill, J.W. Brown, and R.F. Verhey, Complex Variables and Applications, 3rd. Ed., McGraw-Hill Book Company, New York, (1976).

35. A.H. Benade, Acoustics of Musical Instruments, Oxford University Press, New York (1976).

36. C.R. Wylie, and L.C. Barrett, Advanced Engineering Mathematics, 5th Ed., McGraw-Hill Book Company, New York, (1982).

37. R.V. Churchill, and J.W. Brown, Fourier Series and Boundary Value Problems, McGraw-Hill Book Company, New York, (1978).

38. R.E. Edwards, Fourier Series, A Modern Introduction, Vol. 1, Holt Rinehart and Winston Inc., New York, (1967).

39. G.P. Tolstov, Fourier Series, Prentice-Hall Inc., Englewood Cliffs, New Jersey, (1962).

40. A. Papoulis, Probability, Random Variables, and Stochastic Processes, 2nd Ed., McGraw-Hill Book Co., New York, (1984).

41. S.K. Stein, Calculus and Analytic Geometry, McGraw-Hill Book Company, New York, (1973).

42. J.S. Bendat, and A.G. Piersol, Engineering Applications of Correlation and Spectral Analysis, John Wiley and Sons, New York, (1980).